

The Library of High-Precision Simulators

Currently, when drilling is widely used drilling Control Units, which allows using the measured parameters and simulators (mat process models) operatively to determine the parameters and mode of operations, are associated with the optimization and drilling safety. Proposed the creation of a library of simulators based on the numerical solution of complex mathematical models (as usually a system of differential Equations) using the on-board computer. It will allow preventing blowouts and well explosions, which usually cause human losses, damage to environment and are hard and expensive to suppress. We created and developed the Library of simulators very high precision much better then now usually using, allow to significantly be decreasing possibility of accidents while drilling and to accelerate borehole building and significantly increase efficiency and safety of drilling.



Simon Tseytlin has the Doctor of Sc. Degree of Petroleum Engineering. He was graduated from MIFI with Master Degree in Physic and MGU with Master Degree of Mathematic. He got from Aero Space Department of MFTI PhD in Physics. He has strong experience and expertise in creation of Technologies and Software connecting Oil-Gas Industry.



978-613-9-41899-2

Globe
EDIT

Globe
EDIT



Simon Tseytlin · David Tseytlin

The Library of High-Precision Simulators

(Astrophysical Article) On the Origin of Earth and Planets Magnetic Fields

Simon Tseytlin
David Tseytlin

The Library of High-Precision Simulators

FOR AUTHOR USE ONLY

FOR AUTHOR USE ONLY

Simon Tseytlin
David Tseytlin

The Library of High-Precision Simulators

**(Astrophysical Article) On the Origin of Earth and
Planets Magnetic Fields**

FOR AUTHOR USE ONLY

GlobeEdit

Imprint

Any brand names and product names mentioned in this book are subject to trademark, brand or patent protection and are trademarks or registered trademarks of their respective holders. The use of brand names, product names, common names, trade names, product descriptions etc. even without a particular marking in this work is in no way to be construed to mean that such names may be regarded as unrestricted in respect of trademark and brand protection legislation and could thus be used by anyone.

Cover image: www.ingimage.com

Publisher:

GlobeEdit

is a trademark of

International Book Market Service Ltd., member of OmniScriptum Publishing Group

17 Meldrum Street, Beau Bassin 71504, Mauritius

Printed at: see last page

ISBN: 978-613-9-41899-2

Copyright © Simon Tseytlin, David Tseytlin

Copyright © 2019 International Book Market Service Ltd., member of OmniScriptum Publishing Group

FOR AUTHOR USE ONLY

The Library of High-Precision Simulators.

Authors: Dr. of Sc. S. Tseytlin, D. Tseytlin (Tseytlin Consulting Inc.)

Contents:

1. Swab/Surge Simulation.....	2
2. Non-Stationary Heat Exchange in Borehole-Formation System During Washing and Cementing of Borehole.....	13
3. Simulation of Pressure Loss in Drilling or Cementing Well Circulative System Based on Two-Power and Polynomial Models Non-Newton of Liquid Rheology.....	16
4. Simulators of EM MWD Telemetry System for Vertical, Horizontal and Inclining Wells.....	18
5. Simulator of Acoustic Navigation.....	30
6. Simulator of non-stationary two-phase filtration in formation for pressures below bubble point, using Musket equations.....	34
7. Simulator system optimization Well-ESP, is operated simultaneously by two layers.....	39
8. Simulator of Borehole-Formation-Rod Pump System Dynamics, including non-homogeneous zones in formation to Horner's method.....	41
9. Simulator of Centrifugal Pump Optimization of Production Regime Using Borehole.....	44
10. Simulator of borehole-Formation-Choke System Dynamics, applied to layered formation testing.....	45

Attachment (Appendix I)

(Astrophysical Article) «On the Origin of Earth and Planets Magnetic Fields».....	47
---	----

Introduction

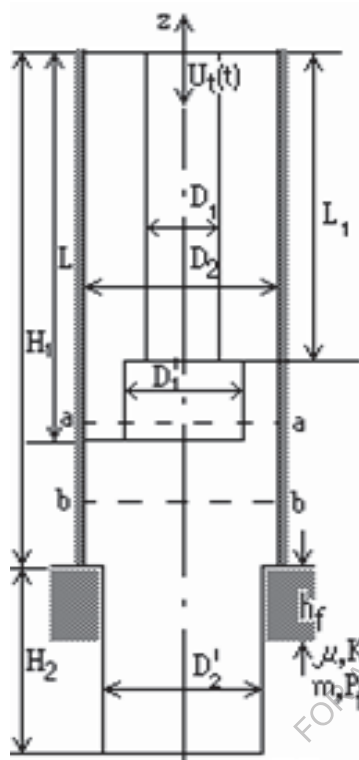
Currently, when drilling is widely used drilling Control Units, which allows using the measured parameters and simulators (mat process models) operatively to determine the parameters and mode of operations, are associated with the optimization and drilling safety. Proposed the creation of a library of simulators based on the numerical solution of complex mathematical models (as usually a system of differential Equations) using the on-board computer. It will allow preventing blowouts and well explosions, which usually cause human losses, damage to environment and are hard and expensive to suppress. We created and developed the Library of simulators very high precision much better then now usually using, allow to significantly be decreasing possibility of accidents while drilling and to accelerate borehole building and significantly increase efficiency and safety of drilling.

In present article we will introduce with some from its.

1. Swab/Surge Simulation.

Simulator of Swab/Surge Tripping Operations, which allows to determine hydrodynamic component of pressure at any point in borehole during tripping, accounting for borehole geometry and moving column composition, fluid compressibility (with borehole walls elasticity), mud features and rheology, moving column velocity, acceleration and deceleration. Simulator allows to determine optimal mode of column tripping in order to decrease hydraulic fracturing risk, invasion zone. Previously same simulators assumed tubes velocity is constant, fluid are no compressibility and Newton liquid. Really that assumes significantly reduce precision of calculations pressure distribution along well walls.

One dimensional math model for to determine hydrodynamic component of pressure at any point in borehole during tripping operations (Fig. 1).



$$\begin{cases} \frac{\partial P}{\partial t} = -\frac{\rho C_i^2}{f_i} \frac{\partial q}{\partial z} \\ \frac{\partial q}{\partial t} = -\frac{f_i}{r} \left[\frac{\partial P}{\partial z} - \left(\frac{\partial P}{\partial z} \right)_{\text{fric}} \right] \end{cases}$$

$$P(z=H, t) = P_{\text{atm}}$$

$$q(z=0, t) = 0$$

$$V[r=D_1/2, t] = U_t(t)$$

$$V[r=D_2/2, t] = 0$$

$$q_k + q_{\text{fric}} + q_d = \frac{\pi}{4} (D_1')^2 U_t(t)$$

$$Re^* = \frac{D^n \rho V^{2-n}}{K \delta^{n-1}}$$

$$\mu c m \frac{\partial P}{\partial t} = \frac{1}{r} \frac{\partial}{\partial r} (r K \frac{\partial P}{\partial r})$$

Fig. 1

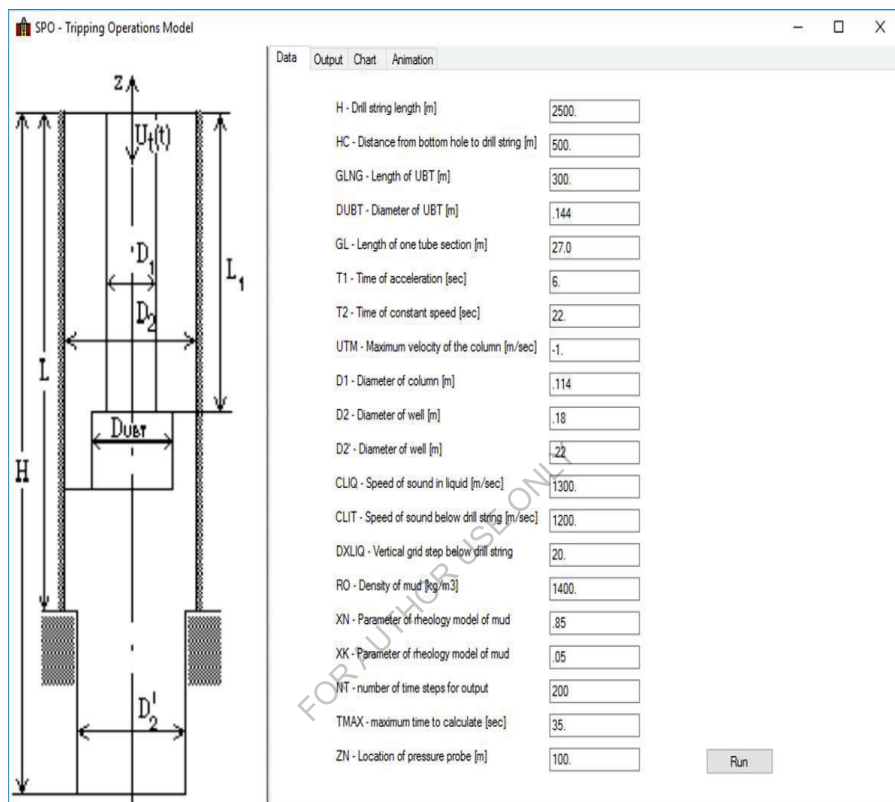


Fig.2
Screen with data of Simulator

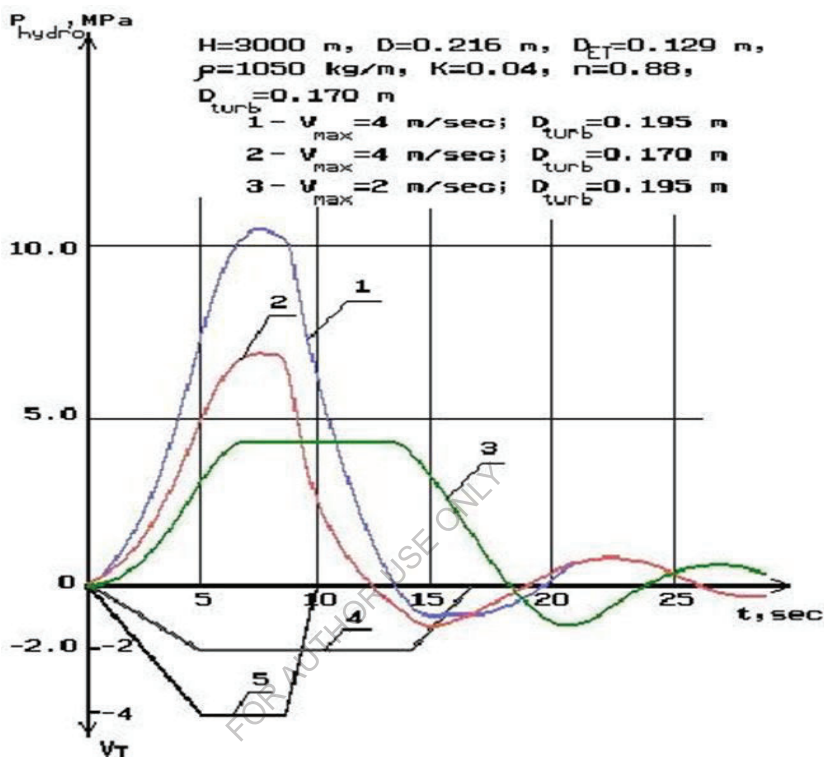


Fig.3

Fig. 3 shows examples of simulation different cases tripping column of tubes for different velocities, sizes and accelerations of tubes. $P(t)=F(V_{max}, D_{tub})$

Below on Fig.4 a, b, c, d shown results of simulations of pressures, volume speeds along well walls for different times.

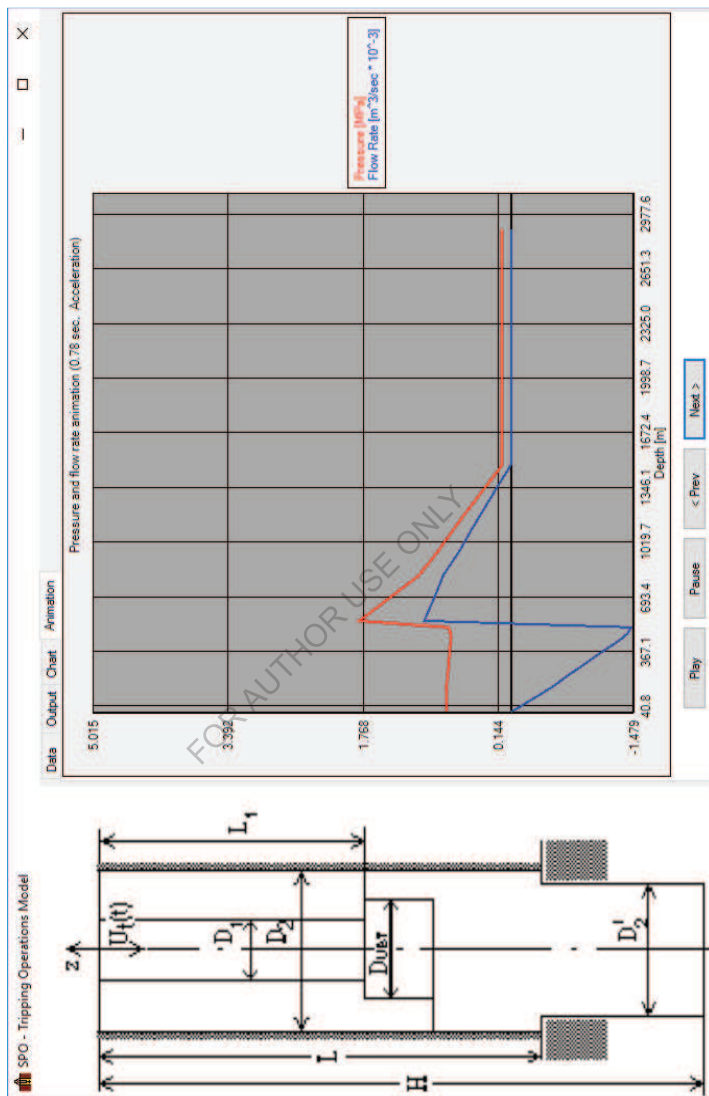


Fig. 4a

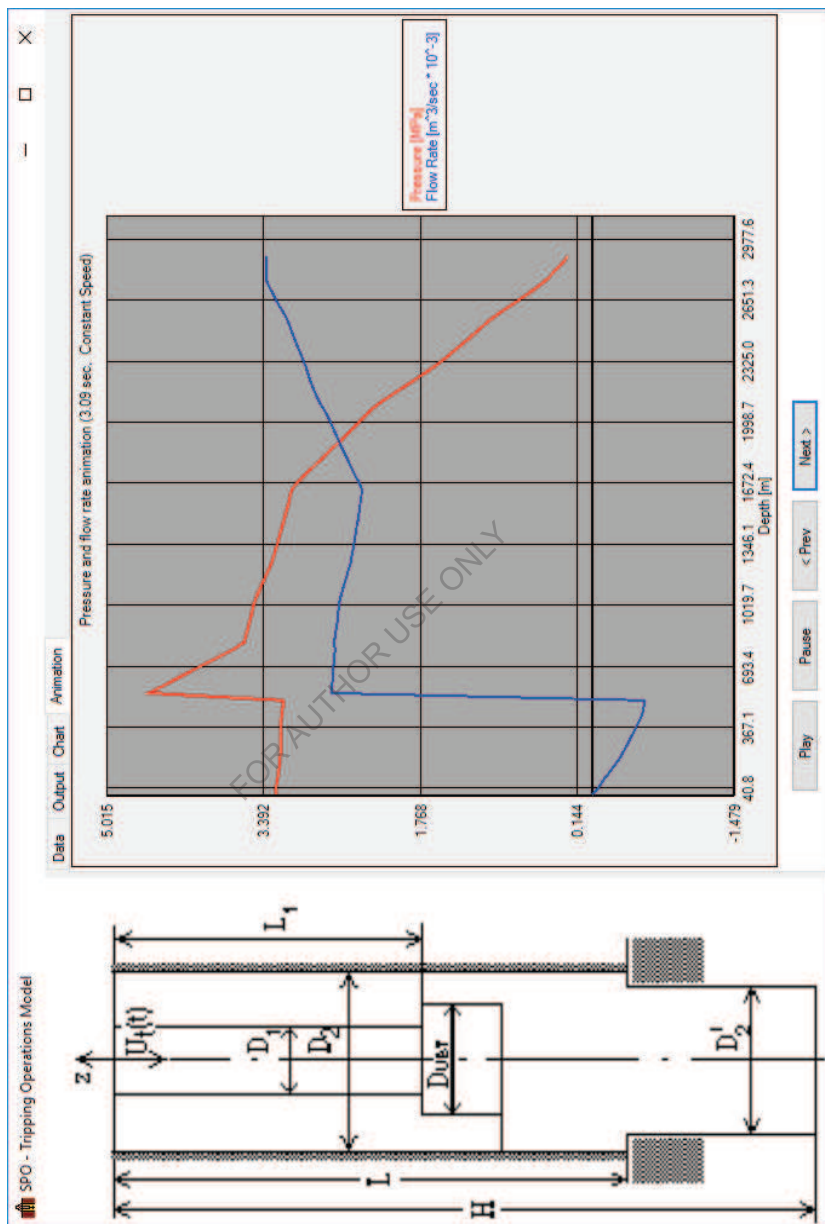


Fig. 4b

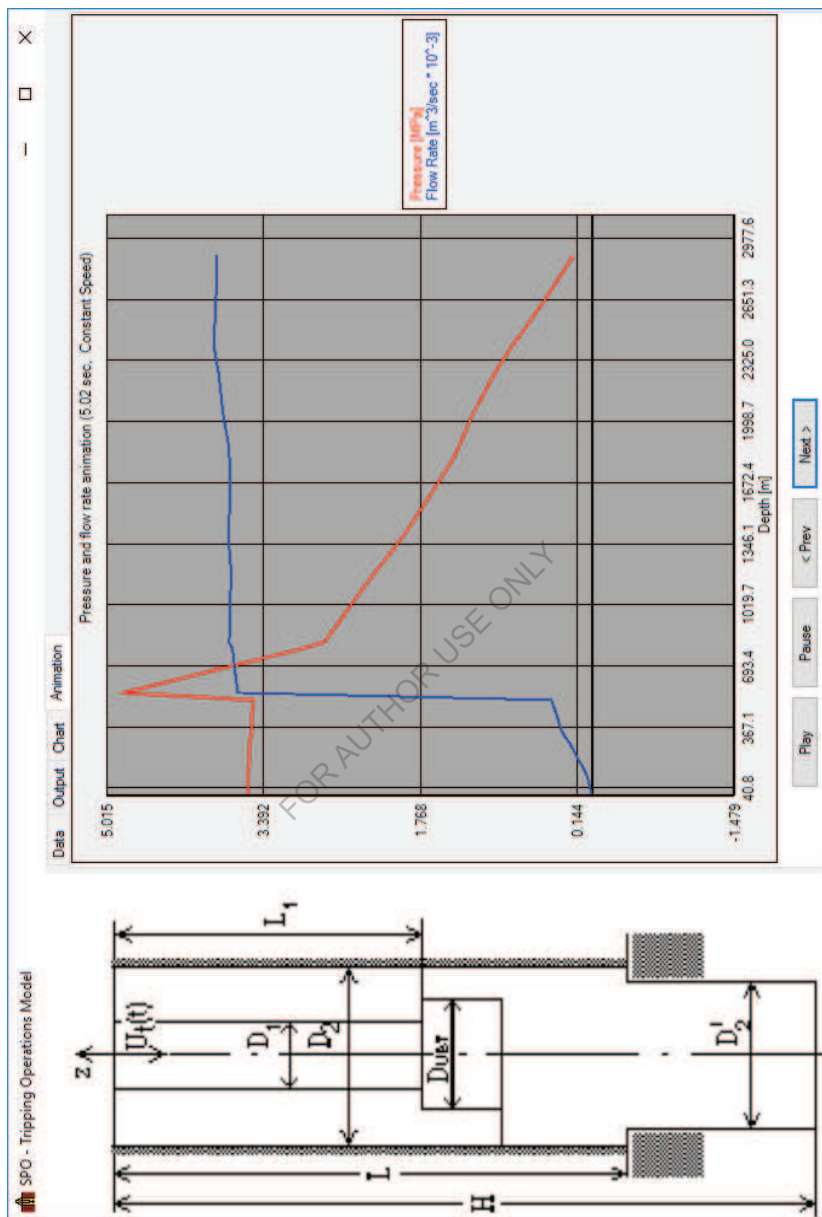


Fig. 4c

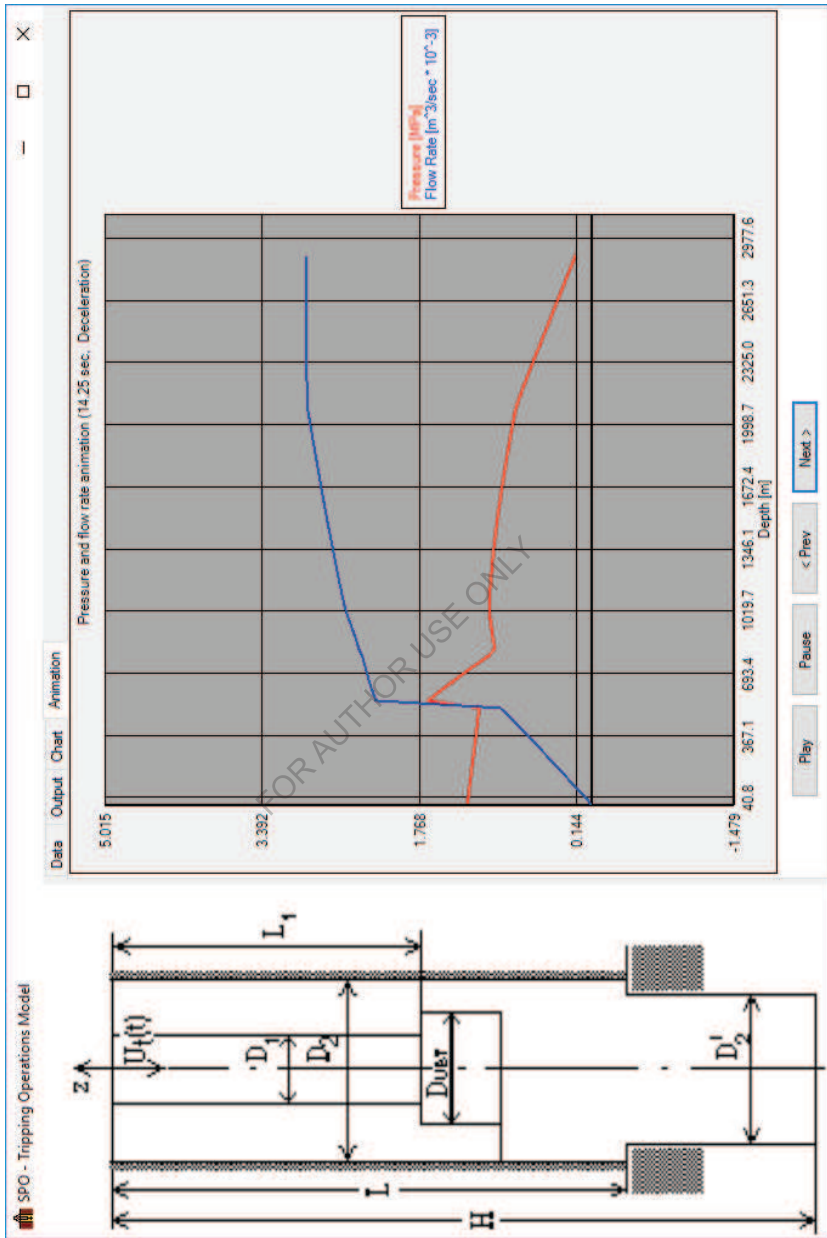


Fig. 4d

Was developed also two-dimensional simulator. Show shortly about theoretical model, which we used (Naiver- Stoke equations for Non- Newton liquid) (Fig. 5).

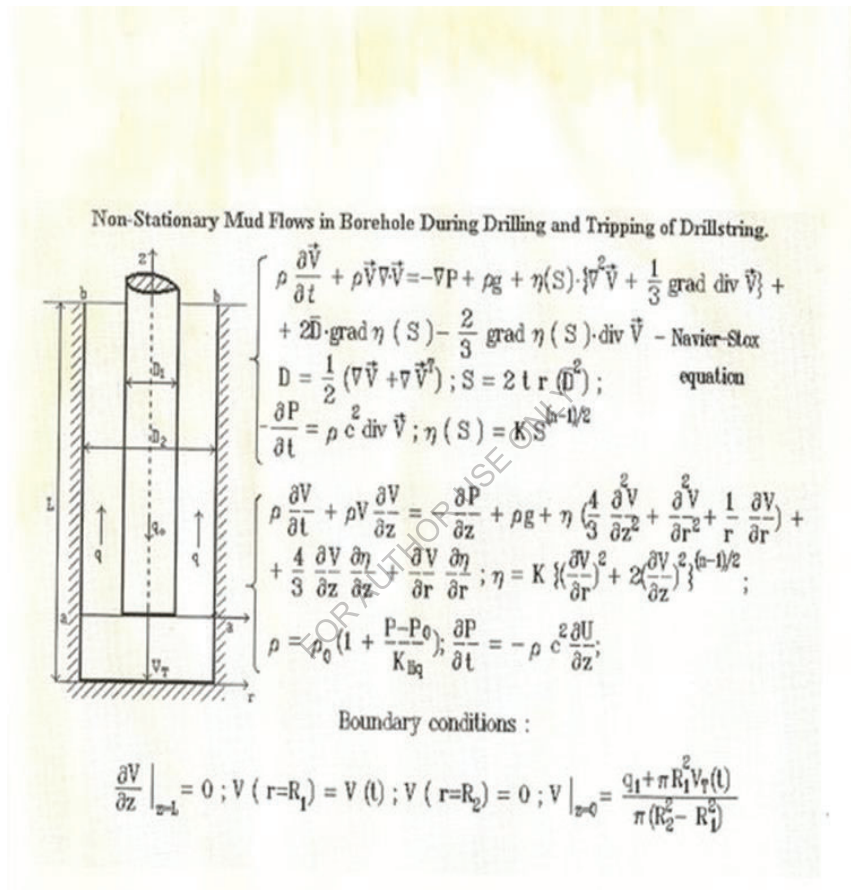


Fig. 5

We also made experiments, which proved right proposed theory.

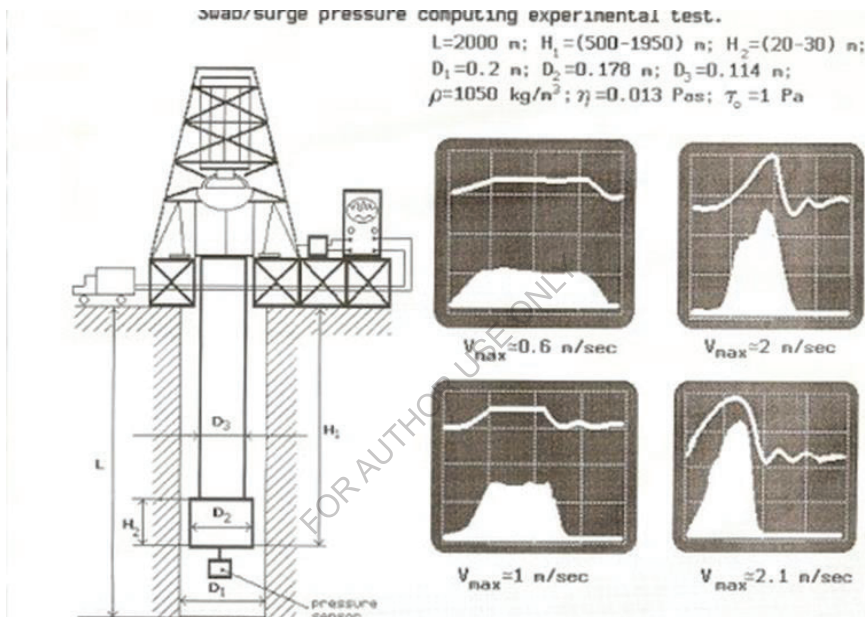


Fig. 6

Fig. 6 shows some results experimental studies swab/surge actions

Conclusions and observations after using swab simulator for different scenarios:

Of great importance is study of dynamic processes arising in a borehole during tripping operations with drill strings while prospecting or production wells are in drill. Tripping operations may cause excessive hydrodynamic loads upon wells walls entailing undesirable hydraulic fracturing and gas kicks which in their turn may cause blowout and uncontrolled fountain. Tripping operations may also bring enlarging of invasion zones and formation clogging in their turn. This worsens logging conditions, cementing quality and makes putting a reservoir into operation more difficult.

Now available methods of computations of hydrodynamic pressure caused by tripping operations do not ensure satisfactory accuracy because they do not account at all or partly such important effects as:

- 1) tripping processes being non-stationary,
- 2) compressibility and non-Newtonian properties of liquids,
- 3) well geometry and drill string arrangement.

Some general regularities may be noted which are concluded from a number of computations for different models:

- 1) Positive pressure maximum is formed near drill string butt-end after acceleration period;
- 2) a minimum of pressure hydrodynamic component may reach negative values (without hydrodynamic pressure) and occurs during a deceleration period;
- 3) a magnitude of the minimum depends on a phase of deceleration begin in relation to a phase of oscillations arising during previous acceleration period;
- 4) pressure maximum depends not only on drill string velocity but also on acceleration; it is a reason not to use methods based on stationary models;
- 5) Mud rheology and density, clearance between a well wall and drill string, drill string velocity and acceleration, possible resonance effects and drill string length have a noticeable influence on the hydro impulse magnitude.

6) Experiments shown good matching with simulation results.

All this effect was considered during the new, more precision simulator of computation.

2. Non-Stationary Heat Exchange in Borehole-Formation System During Washing and Cementing of Borehole.

The Simulator of Heat Exchange in Borehole-Formation System, which allows computing temperature changes in drilling tubes, annular space and surrounding rocks during washing and cementing. It accounts for changes with depth in geometry of drilling tubes and borehole, mud properties and volumetric rate, thermos physical properties and geothermal coefficient of rocks surrounding borehole, presence of formation with changed thermos physical parameters of the rock. The simulator allows quick and precise determination of the temperature distribution in the system, depending on a number of system parameters at any time; it is necessary for borehole monitoring. It can prevent a number of dangerous complications and takes into account temperature influence on mud and cement properties during the borehole washing and cementing. A numerical axisymmetric problem of unsteady heat exchange between formations and a vertical well with circulating mud in it, geothermal gradient change versus depth, thermal parameters of surrounding formations, heat exchange coefficients versus temperature, channel geometry and liquid rheology being considered. To do so the whole channel length was divided into intervals within which tubes and well sections together with adjacent formation thermal properties and mud rheology were or were regarded to be constant. For each such interval a system of differential equations may be offered to describe it:

λ	Γ	X
Wt/m-sec	deg/m	m ² /sec

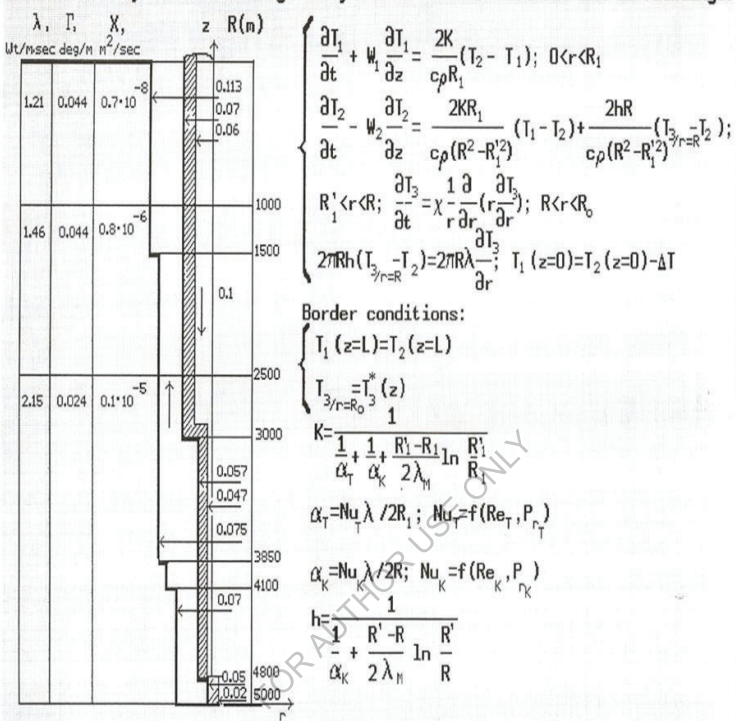


Fig. 7

Temperature Distribution Calculation in the Drilling Tube, the Annular Space and the Surrounding formations at Different Time While Drilling and Cementing.		
R1 = 0.068	drilling tube radius	[M]
R = 0.112	borehole inside radius	[M]
DL = 3000	borehole depth	[M]
Q = 0.009	volumetric flow rate	[M ³ /sec]
NU = 0.040	mude viscosity	[Pa*sec]
TAU0 = 4.100	starting shift stress	[Pa]
RO = 1240	density	[Kg/M ³]
C = 4200	heat capacity	[Dg/Kg*grad]
HR = 0.040	radius step in formation	[M]
LAM = 0.750	mude temp.conductivity	[Wt/M*grad]
AKK = 0.150,0.150,0.150,0.150,0.150	temperature conductivity	[M/sec ² *10 ⁻⁶]
DDP = 0.600,1.200,1.800,2.400,5.000	thermal conduct. of form.	[Wt/M*grad]
LL = 500, 1000, 2000, 2500, 3000	down border of formation	[M]
G = .0100,.0200,.0300,.0150,.0600	thermal gradient	[grad/M]
TMAX= 3600	maximum time of solution	[sec]
DDDT= 180	time step for output	[sec]
Press ←,→,↑,↓to select,<Enter> to change,<Tab> to start,<F10> to exit		

Fig. 8, Screen with data of model

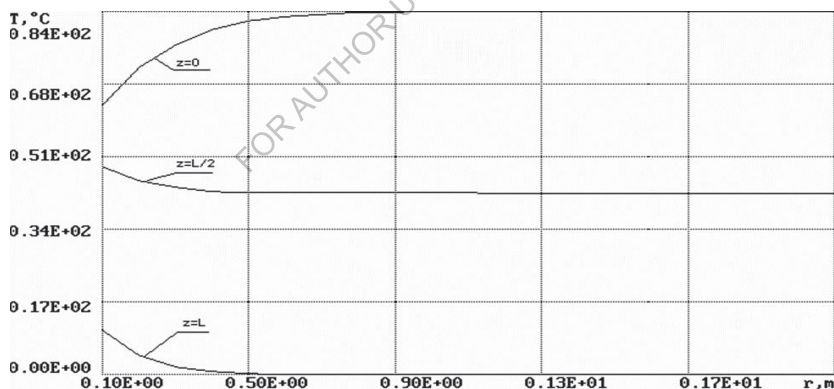


Fig.9. Temperature distributions inside surrounded well formation $T(z, r, t)$

Non-Stationary Heat Exchange in Borehole-Formation System During Washing and Cementing of Borehole.

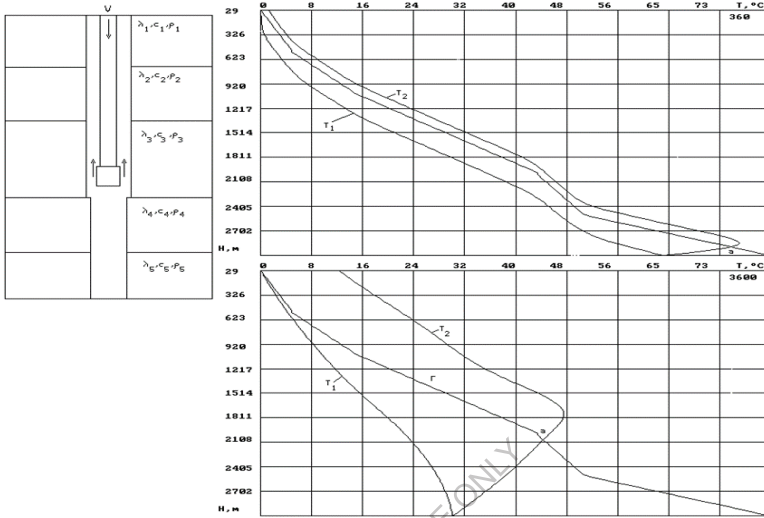


Fig. 10. Results simulation temperature distributions $T(z, t)$ inside drill string, annular space and natural gradient for two times 360 and 3600 sec

3. Simulation of Pressure Loss in Drilling or Cementing Well Circulative System Based on Two-Power and Polynomial Models Non-Newton of Liquid Rheology

The simulator allows to calculate pressure losses in borehole during drilling and cementing. Approximation of rheological characteristic measured by viscos meter with two-power and polynomial model of non-Newtonian liquid, provides best precision among similar methods of pressure computation, because the polynomial model in computations uses full information received from multi velocity viscos meters. Z-criterion usually used for a non-Newtonian liquid power model is used in the simulator for determining the flow type. After the borehole circulating system channel is presented as the tube sections of round and annular profile with a constant area, their flow type is determined. Then simulator

computes pressure losses for two-power and polynomial models of liquid flow. Precision benefits from using polynomial model are most significant for high viscosity muds with complicated rheology.

Circulation of Pressure Loss in Circulative System of Well Based on Two-Power and Polynomial Rheology Model

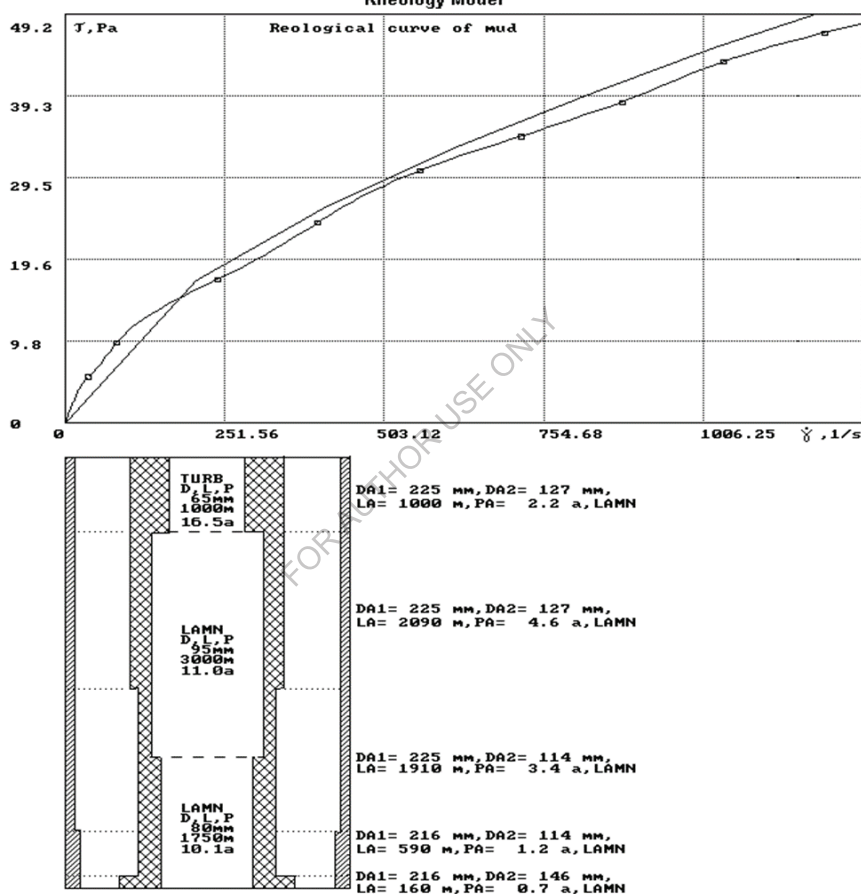


Fig.11

4. Simulators of EM MWD Telemetry System for Vertical, Horizontal and Inclining Wells

Our EMMWD Simulators allows you to simulate performance of your specific existing or anticipated tool configuration(s) and to run the model for a wide range of various scenarios, e.g. just vertical wells, inclined wells, or wells with horizontal section, multiple formations with different resistivity and permeability values, influence of the drilling fluid, different types of transmitters, receivers, and gaps configuration, accounts for effect of different casing and drill string configurations, finite resistance and permeability of metal and drill string joints, etc. (Fig. 12)

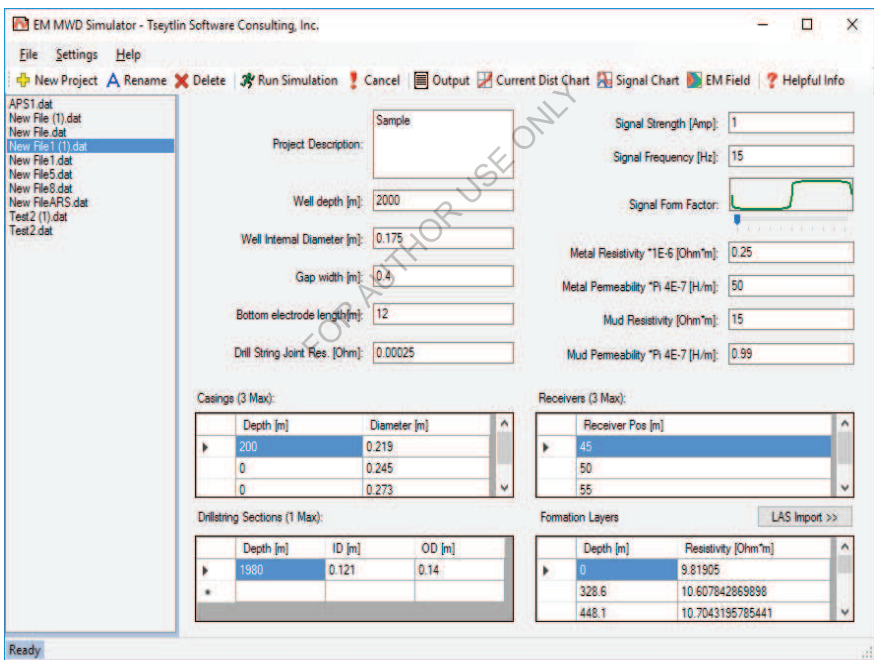


Fig. 12. Screen for specifying the parameters of the simulator

Our EMMWD simulators have allowed also to answer a number of important questions, related to the system design and physics of different phenomena observed in the process of operation of EM MWD systems, as:

1. Compute signal attenuation based on properties of the rock, mud, characteristics of the drilling pipes, signal frequency, etc. (Fig. 13)
2. Pick optimal signal strength and frequency based on certain parameters of different system components.
3. Determine all electromagnetic parameters and distributions, including E , H , j , U in the surrounding rock and along the drill string.
4. Calculate impedance of the whole system.
5. Determine the optimal gap size.
6. Determine the best drilling fluid.
7. Determine parameters of the receiver.
8. Simulate magnitude, shape, phase shift, and dispersion effects for the signal acquired at the surface.
9. Can serve as a demo and / or a marketing tool for the clients.
10. Can evaluate suitability well for EMMWD technique
11. Attached to your EMMWD tools relevant high precision simulators, can increase the attractiveness and price of EMMWD tools.

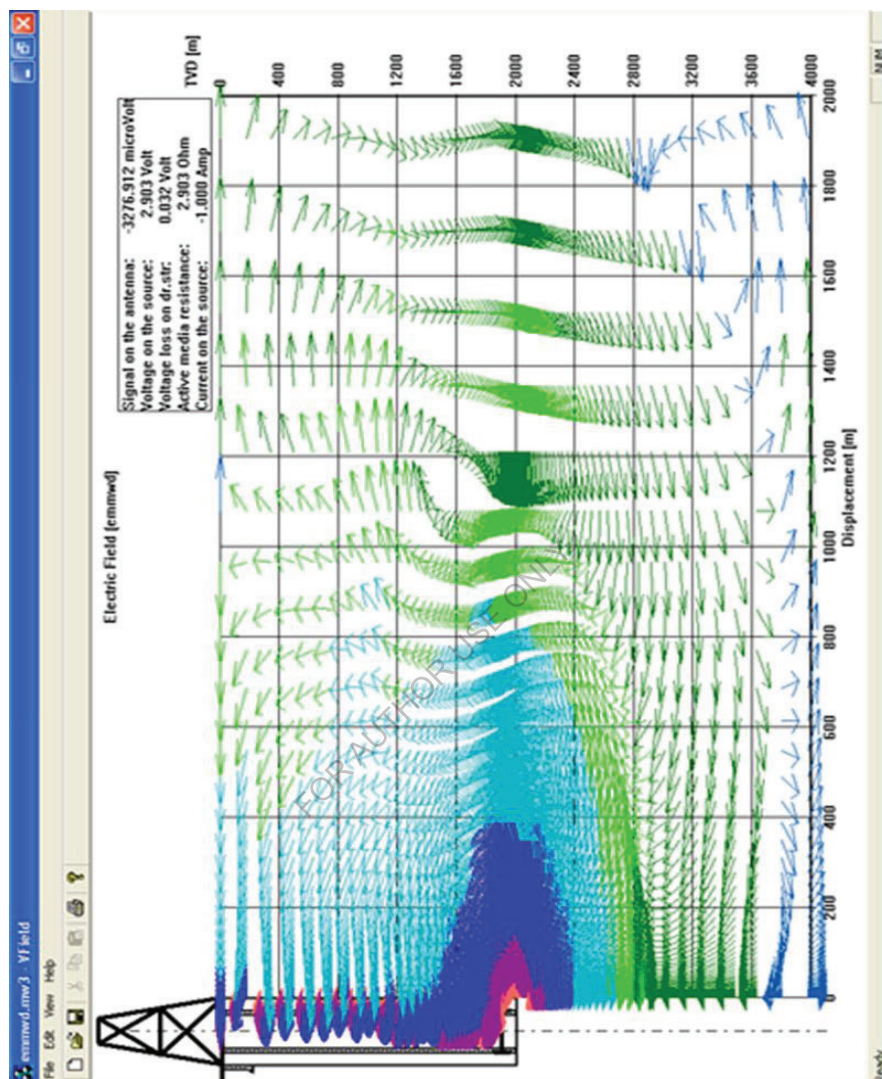


Fig. 13
Electric Field

Propagation of electromagnetic signals through this system is core of EMMWD Simulators by the full system of Maxwell equations in addition to the Ohm's law:

$$\left\{ \begin{array}{l} \operatorname{div} \vec{E} = \frac{\rho(t, \vec{x})}{\varepsilon} \\ \operatorname{rot} \vec{E} = -\frac{\partial \vec{H}}{\partial t} \\ \operatorname{div} \vec{H} = 0 \\ \operatorname{rot} \vec{H} = \mu \vec{j}(t, x) + \varepsilon \mu \frac{\partial \vec{E}}{\partial t} \end{array} \right. \quad \vec{j} = \sigma(t, \vec{x}) \cdot \vec{E}$$

Where H-magnetic field intensity, E-electric field intensity, j-current density.

EM MWD Simulator

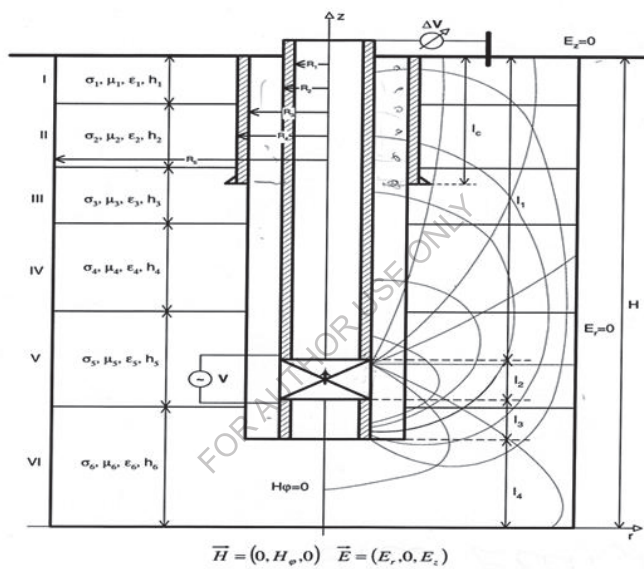


Fig. 14, Field of problem solution

Below shown few screens our Simulators:

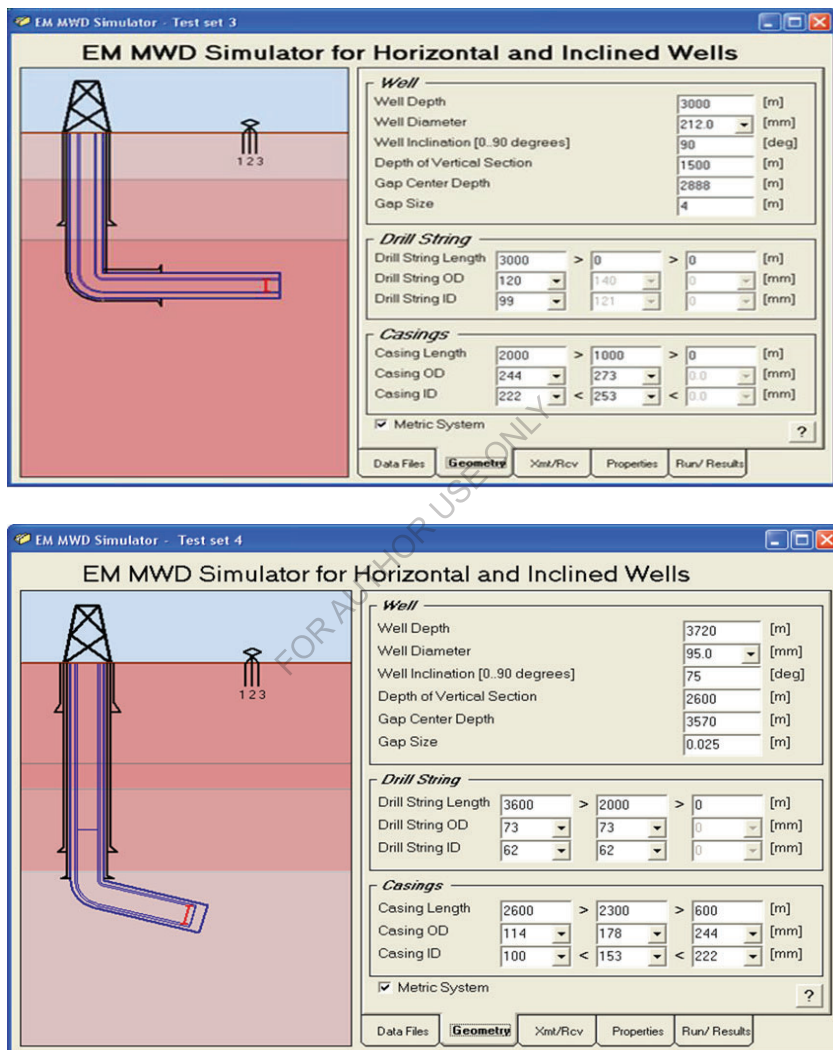


Fig.15 a, b, some data screens

Our EMMWD Simulators contains possibilities for Import Resistance Log in. The application can load LAS-format files containing formation resistance log information.

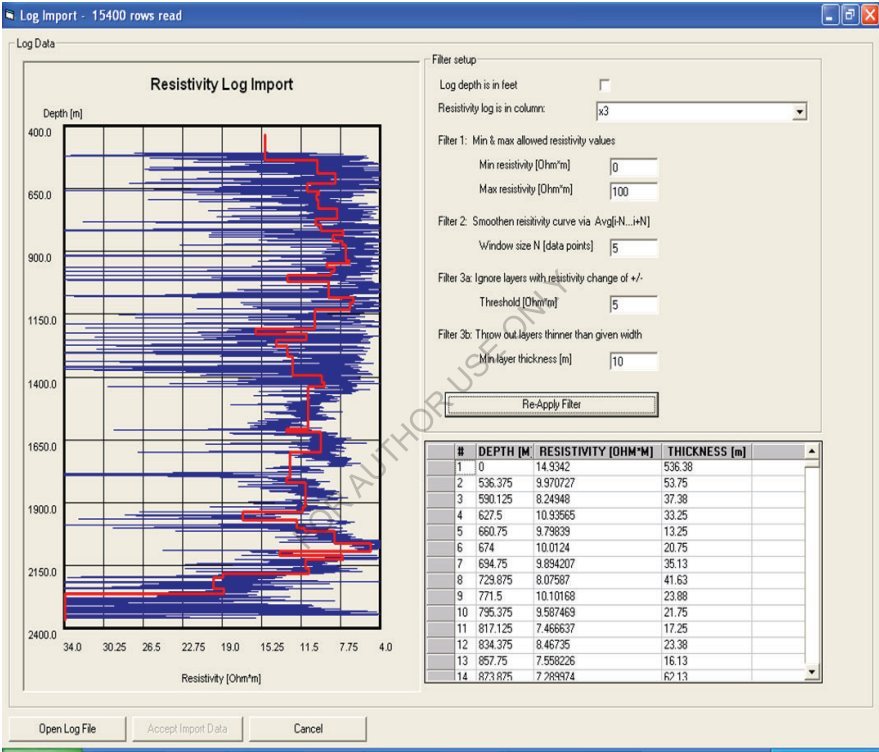


Fig. 16

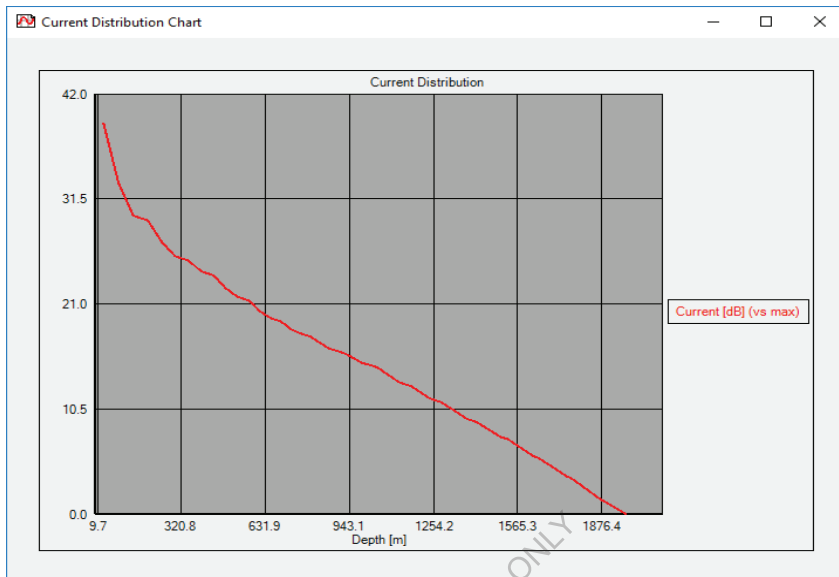


Fig. 17, Current distribution along drilling tube

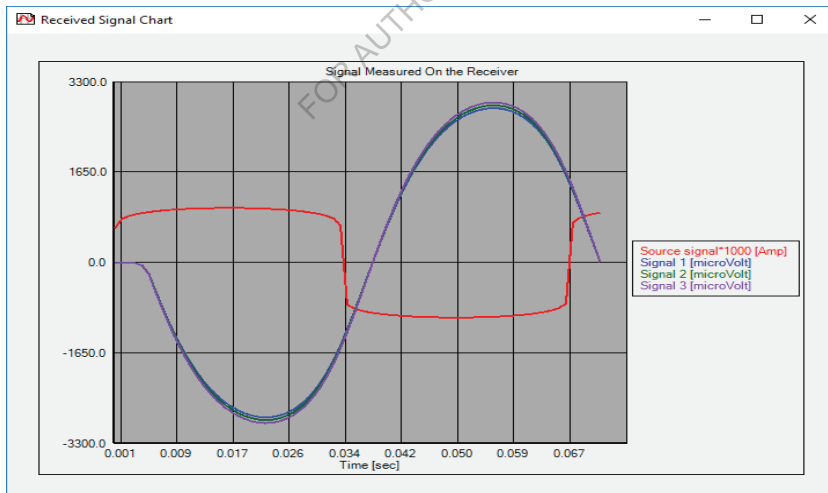


Fig. 18, Signals of source and receivers

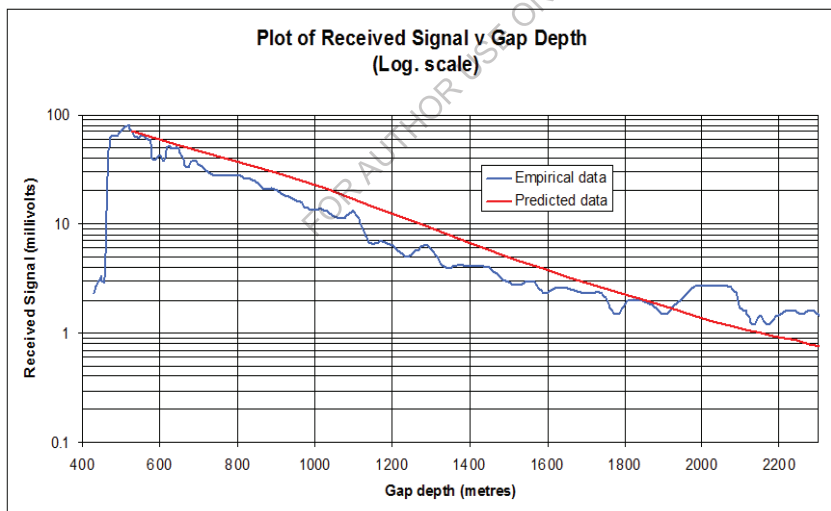
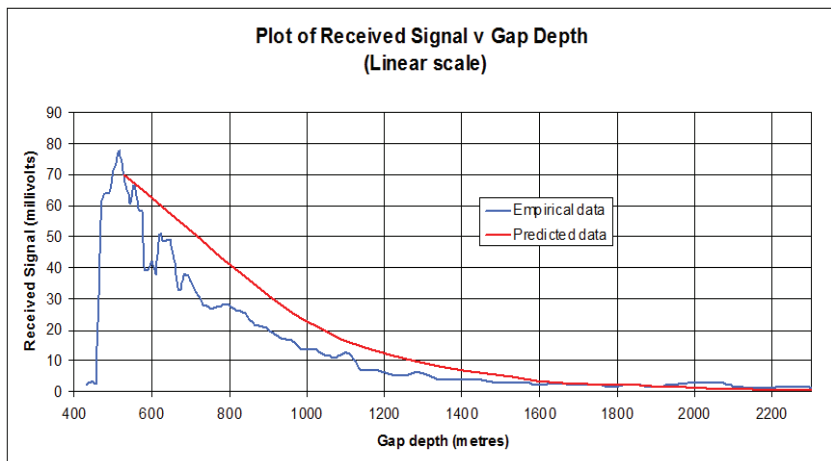


Fig. 19. Examples good matching results simulation and measured

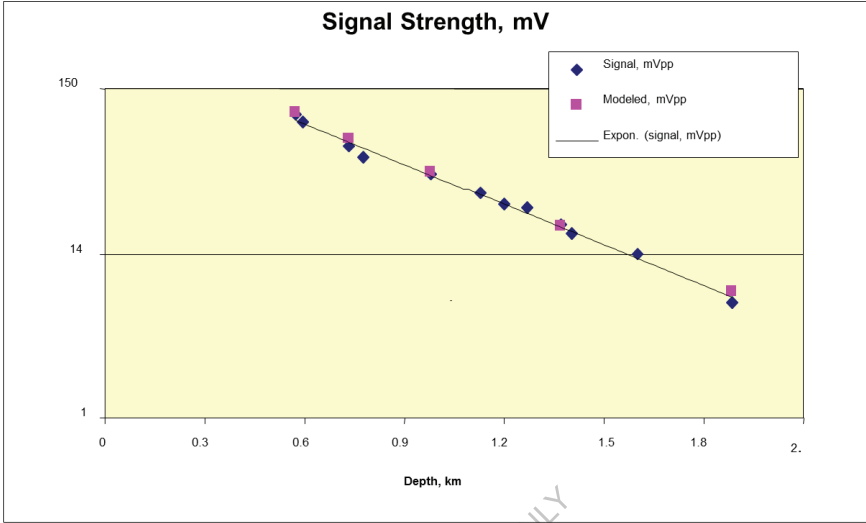


Fig. 20, Good matching results

Observations, Conclusion.

A number of interesting phenomena were observed in the process of solving this problem. These observations could help better understand the physics of the EMMWD system in general and the influence of various system and environmental components. This knowledge can be also useful for optimal system design and for better understanding of the acquired signals' parameters during operation.

Here is a brief summary of the most important observations along with corresponding conclusions and recommendations:

1. the most important parameter, which was calculated by using the simulator, is the equivalent impedance of the surrounding media. This impedance largely depends on the resistivity of the drilling mud, formation conductivity and the size of the gap. Therefore, the size of the gap can be optimally selected based on the other [environmental and geometrical] parameters' values.

2. The level of the signal acquired at the surface noticeably depends on the current emitted by the tool into the media. Therefore, the downhole dipole source should be a “controlled current” type of source rather than a “fixed voltage” source.

3. Presence of the casings affects the properties of the signals detected at the surface by enhancing their magnitudes. However, the significant effect takes place only if fairly long casings are used.

4. Lines of the electrical field vector (E) and the current (J) form a contour (loop), which starts at one electrode of the downhole dipole electric source and ends at the other one. However, every half-a-period, when the signal polarity switches to the opposite one, the electrical field lines change the direction as well. Therefore, the eddy currents are being formed; these currents are then moving (diffuse) into the peripheral areas. Rate of diffusion depends on both the electric-physical properties of the media and the electric field gradient. This causes distortion of the electric field lines in the layers with different conductivity. The higher the layer's resistance, the greater the diffusion rate is. This is why the electric field lines in the highly conductive layers slow down, as in the less conductive they take a lead.

5. Metal pipes are characterized by certain finite value of the electrical impedance, which consists of both active and reactive resistance components. The active component depends on the metal conductivity, cross-sectional area of the pipe, and the pipe joints' resistance. This component significantly affects level of the signal received at the surface. Reactive component is primarily defined by the inductance of the pipes. This is why it's better to use pipes with minimal value of magnetic permeability. The inductive resistance depends on the frequency; it starts to affect the signal at higher frequencies. However, if the transmitter pulses have steep fronts, the inductive resistance of the drill string can significantly disturb the signal due to dispersion effect and greater attenuation at higher frequencies.

6. Inductance of the drill string causes some phase shift in the signals measured near the wellhead. If the signal is measured by the probes

(antenna) further away from the wellhead, an additional phase shift may occur due to the finite value of the diffusion rate of the electromagnetic field, which in turn depends on the conductivity of the formation. This rate of diffusion may reach from several hundreds to a thousand meters per second.

7. Increase in the diameter of the drill string and the thickness of the pipe wall decreases attenuation of the signal propagated to the surface.

8. Increase in the resistivity of the drilling mud decreases signal attenuation. For a water-based or another conductive type of mud the gap needs to be increased and may reach up to 20 m or so to ensure efficient signal transmission.

9. The length of the lower electrode of the downhole transmitter affects the total impedance of the system, such as both the current density and the electrical fields have the highest values near its surface. It is not recommended to have the lower transmitter electrode shorter than 10 m, since it may increase signal attenuation.

10. If the signal frequency is relatively high (e.g., 10 Hz or higher) and the signal shape at the source is close to the square pulse, the signal acquired at the surface will look like the first harmonic of the transmitted signal. Higher signal harmonics (i.e. 20, 40, 80, Hz) will be significantly attenuated before they reach the surface of the earth.

11. When a highly resistive mud is used (resistivity > 100 ohm-m), the effect of the actual conductivity of the surrounding formation is diminished. In this case abrupt changes in the curve of the current distribution along the drill column are not observed, unlike other cases. Signal attenuation in this case is usually significantly reduced.

5. Simulator of Acoustic Navigation

When drilling is stopped (or while drilling), the acoustic source, mounted on a drill string, generates a pressure pulse. This excites both tube waves within the borehole and acoustic waves in surrounding formation. The resulting acoustic waves propagate through the formation, experiencing partial reflection on existing acoustic boundaries. Upon reaching borehole walls the reflected waves excite corresponding tube waves, which are being registered by receivers mounted on the drill string. While incident and reflected waves propagate in formation, tube waves propagate within borehole reflecting from stabilizers and the bottom of the hole reception of the informative signal as well as exciting additional waves in formation. (Fig.21a, b,c,d,e,f).

Applications

Acoustic navigation systems are used for determining location of bit relative to formation boundaries during horizontal and directional drilling.

Simulator helps studying physical processes and interpreting the measurement results.

Determine requirements to the source and receivers.

Assists in finding the optimal parameters of the tool.

Optimize relative locations of transmitter and receiver to minimize signal disturbance.

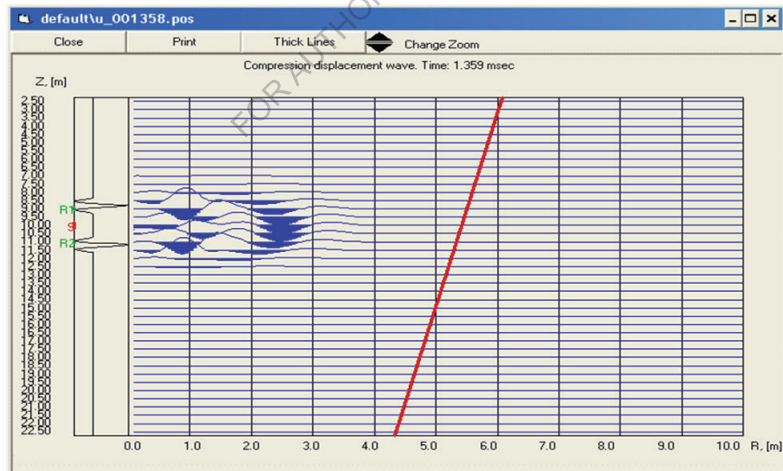
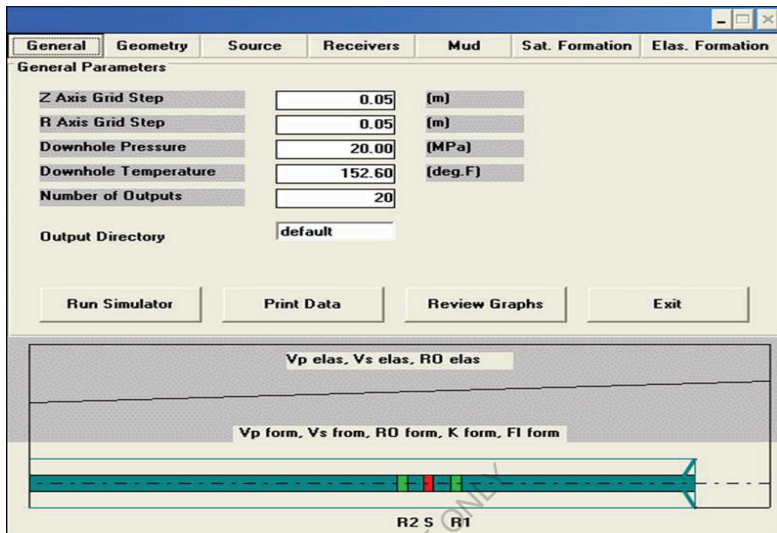


Fig. 21b

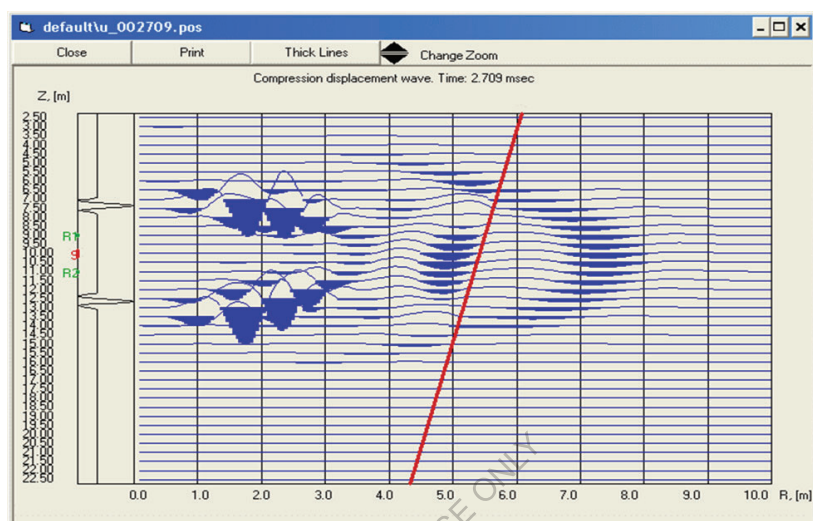


Fig. 21c

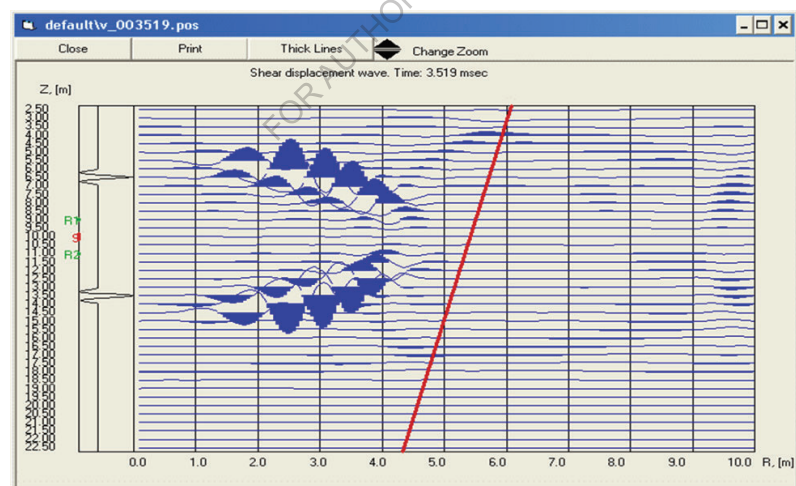


Fig. 21d

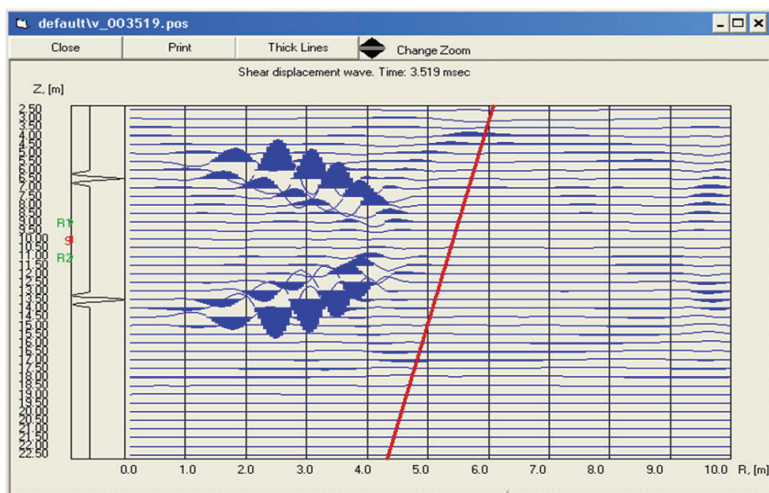


Fig. 21e

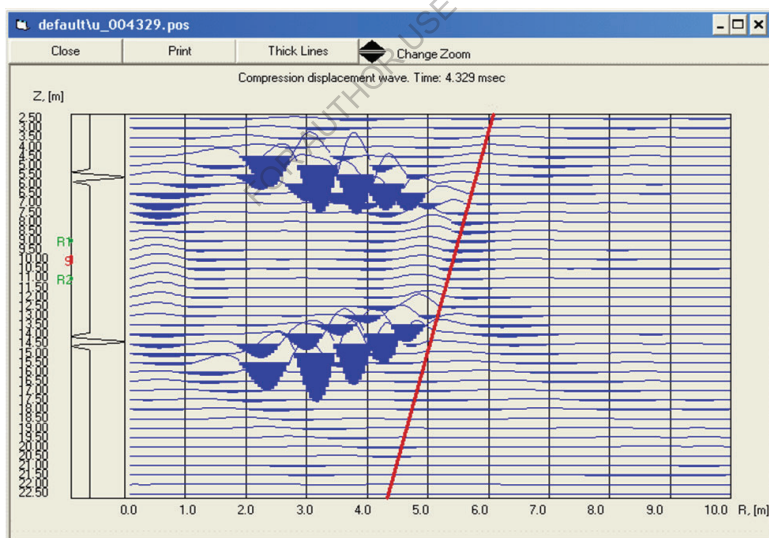


Fig. 21f

6. Simulator of non-stationary two-phase filtration in formation for pressures below bubble point, using Musket equations

This method allows receiving maximum current oil rate, extending life of the well and increasing its oil recovery index by keeping current bottomhole pressure on the optimal level, which is continuously calculated using a special mathematical model, and depends on current properties of the system well-formation and properties of formation and fluid.

Maximum oil rate is achieved by maintaining formation in such a mode, as to minimize negative effects in the bottomhole area, which appear due to free gas, which separates from oil, blocking oil flow, and due to forming of zones of sluggish, viscous degassed oil. Application of this method also decelerates pressure drop in formation by lessening premature exiting of gas from formation and decreases current value of GOR. This leads to extended life of well and increased ultimate production index.

The method applies to all oil production methods, such as fountain, gas-lift and pump, and allows receiving millions of additional barrels of oil without drilling any extra wells or building any additional expensive platforms for offshore wells.

Oil Production Optimization and Enhanced Oil Recovery Method for Formations Containing Oil with High Gas to Oil Ratio.

Pressure, Oil Rate and GOR vs. Oil Recovery

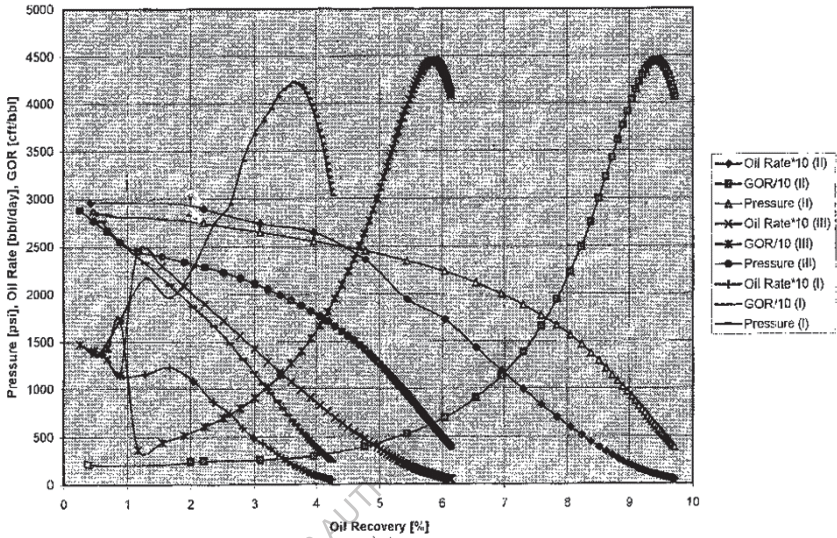


Fig.22

Let's examine a sample application of this method, using mathematical model of processes describing the major mechanisms appearing in formation during non-stationary filtration of two-phase fluid. For that let's employ one-dimensional axis-symmetrical system of Musket equations, with corresponding PVT characteristics of fluid and dependencies of relative permeability K_{ro} , K_{rg} from liquid saturation (S_o):

$$\frac{1}{r} \frac{\partial}{\partial r} \left(r \frac{k_{ro}}{\mu_o B_o} \frac{\partial p}{\partial r} \right) = -158.064 \frac{\phi}{k} \frac{\partial}{\partial t} \left(\frac{S_o}{B_o} \right) \quad (4)$$

$$\frac{1}{r} \frac{\partial}{\partial r} \left[r \left(\frac{k_{rg}}{\mu_g B_g} + \frac{R_g}{5.615} \frac{k_{ro}}{\mu_o B_o} \right) \frac{\partial p}{\partial r} \right] = -158.064 \frac{\phi}{k} \frac{\partial}{\partial t} \left(\frac{S_g}{B_g} + \frac{S_o}{B_o} \frac{R_g}{5.615} \right) \quad (5)$$

Where: $P(r,t)$ – pressure in formation; $S_o(r,t)$ – oil saturation in formation; $S_g(r,t)$ – gas saturation in formation; $R_s(P)$ – solution of gas in oil; $B_o(P)$ – oil formation volume factor; $B_g(P)$ – gas formation volume factor; ϕ – porosity, μ_o – oil viscosity, μ_g – gas, k_{ro} – relative oil permeability, k_{rg} – relative gas permeability.

There was created a corresponding simulator for purposes of analysis and prediction. For example, the following formation was analyzed: radius $R_f=1000$ ft; height $H=50$ ft; $F_I=0.15$; $K=15$ mD, $r_w=0.3$ ft, I – the case when bottomhole pressure was kept at $P_{bot}(t)=0.25 \cdot P_f(t)$; II – the case when bottomhole pressure was kept at $P_{bot}(t)=P_{botopt}(t)$; III – the case when at first for approximately 120 days the well worked according to scenario I, and then it was switched to scenario II.

Behaviors of oil rate (Q_{oil}), formation pressure (P_f), and GOR, in dependence of current recovery index (N) are shown on Fig22. In case I, the well worked for approximately 990 days before the oil rate fell to 6 bar/day, the limit of production sensibility. By that time the well gave $\sim 4.25\%$ ultimate recovery index. In the second case the well worked for 1440 days and gave $\sim 9.8\%$ ultimate recovery index (more than double!). In case III, when the well was switched to optimal regime 120 days after production started, the ultimate oil recovery index increased from 4.25% to $\sim 6.2\%$. At the same time, switching the well into optimal regime reduced GOR and increased oil rate from 130 bar/day to 250 bar/day.

All these positive effects were achieved due to keeping bottom hole pressure at the optimal level, which brought to reduction of forming of oil blocking zone in formation near bottomhole and slowed down loss of gas from formation, which causes formation pressure to drop.

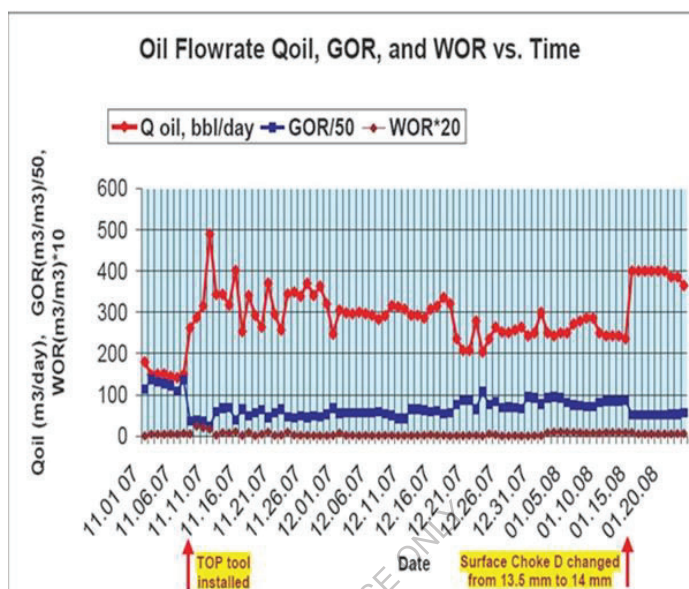


Fig. 23, Example applying TOP technology

Besides the obvious key benefit, i.e. increase in oil production rate, the proposed technology brings numerous additional benefits, such as the following:

- Reduce the current GOR and WOR
- Reduce (or eliminate) gas and water cones
- Decelerate depletion of formation pressure
- Increase ultimate recovery index of the well and the oil field
- Improve stability of well performance
- Avoid premature loss of formation pressure and energy
- Increase life-time of wells
- Eliminate appearance of high viscosity areas in formation near bottom hole zone
- Increase formation's relative permeability coefficient by oil
- Increase productivity index of the formation

- Increase in the efficiency of gas-lift and pumps
- Decrease in electric energy consumed by pumps and gas-lift compressors
- Reduce formation sand washout, mechanical damages to the formation, and formation permeability loss

The Economic Effectiveness of the TOP is achieved due to the combination of all benefits listed above. Overall, it is related to the improved conditions for oil production. The number of wells suitable for potentially beneficial employment of TOP is really huge. This technology can be utilized for all oil production techniques, i.e. flowing, gas-lift, pump, etc. The method can be applied both during development of new oil fields and for improvement of older wells. The economic effect from implementation of this technology can be expressed in terms of getting millions of additional barrels of oil or hundreds of millions of dollars without drilling extra wells or building additional expensive platforms for offshore production

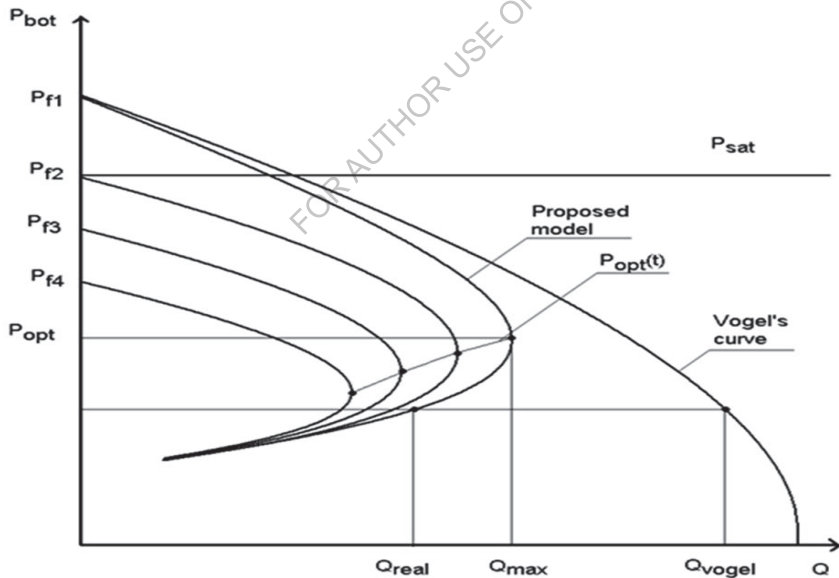


Fig.24, IPR dependence

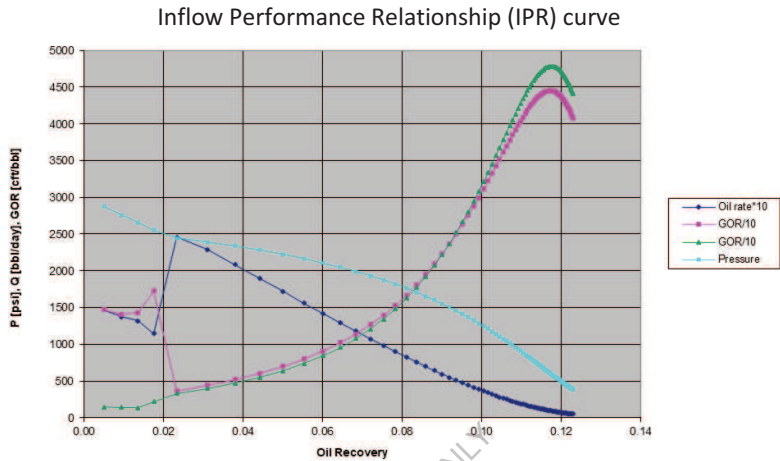


Fig.25

Computer Simulation Results: Rate, Formation Pressure and GOR vs. Oil Recovery

7. Simulator system optimization Well-ESP, is operated simultaneously by two layers

Function and Features Simulator.

Optimum simulator to evaluate the effectiveness of DLA technology to this well. It allows you to define:

- Downhole pressure both layers;
- Their production rates, the total flow well rate, the water content of products;
- Pump head to determine the frequency of the pressure supply pump
- Gas content and pressure at the pump inlet;
- The dynamic level of the well;
- To determine the optimal depth and performance;
- Regulate the downhole pressure and flow rates using hydro resistance;

- Producing analysis of each reservoir separately (for example build up Simulator system optimization Well-ESP, is operated simultaneously by two layers

Function and Features Simulator.

- Optimum simulator to evaluate the effectiveness of DLA technology to this well. It allows you to define:
- Downhole pressure both layers;
- Their production rates, the total flow well rate, the water content of products;
- Pump head to determine the frequency of the pressure supply pump
- Gas content and pressure at the pump inlet;
- The dynamic level of the well;
- To determine the optimal depth and performance;
- Regulate the downhole pressure and flow rates using hydro resistance;
- Producing analysis of each reservoir separately (for example build up test).test).

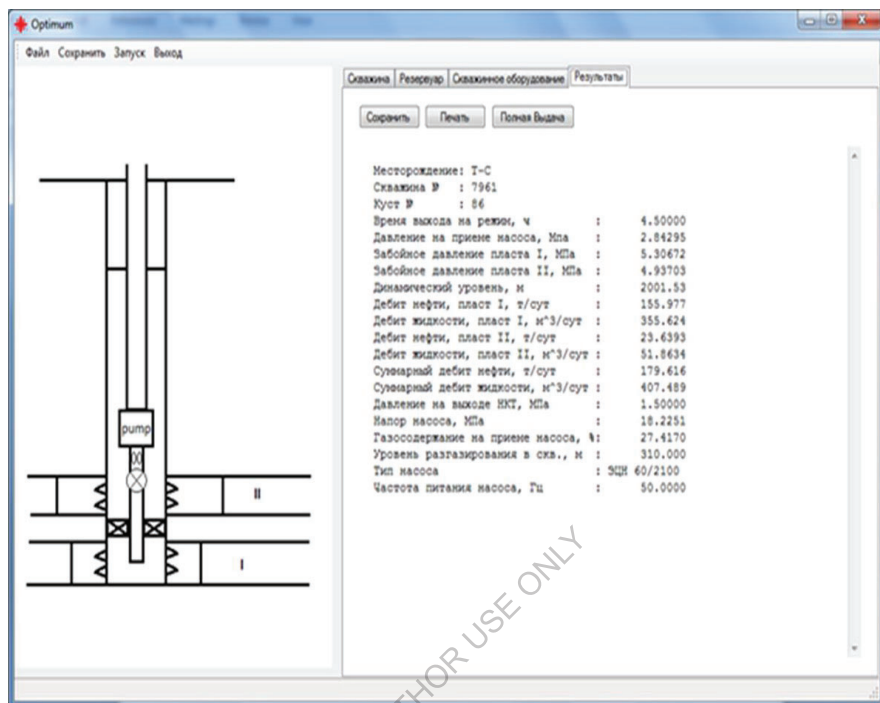


Fig.26, Data Screen

8. Simulator of Borehole-Formation-Rod Pump System Dynamics, including non-homogeneous zones in formation.

The simulator allows accounting for interaction between reservoir of complex structure (layered or fractured) and borehole with multiphase fluid flow. As a rule, the third element of the system is a two-phase choke or a down-hole pump. Such a consideration of the system allows more adequate simulation of processes which take place during formation test or well production.

A group-of-reservoirs-borehole-choke simulator has about 30 parameters controlling its elements. It allows investigating and creating methods for well production tests, for testers on tubing or logging cable accounting for their specific features. The simulator allows investigation of influence of 1) reservoir properties

upon apparent permeability, 2) degassing of oil in the zone near a borehole upon phase permeability, 3) perforation quality and extent upon results of measuring, 4) interflows between layers upon measuring, 5) presence of high permeability layer upon depression value near bottom, 6) presence of choke upon functioning of the whole system etc.

The same simulator allows to investigate the processes which take place on fountain production of a well in order to find an optimum regime of its exploitation to increase production of the well by means of changing choke diameter, proper perforation and flow rate. The simulator may also be used for theoretical researches bound with injection wells and hydraulic fracturing.

The solution is presented in graphical form on the screen being a set of isobars inside a reservoir, diagrams of bottom hole pressure and flow versus time. Optionally user can enable transit pressure curves to Simulator of Borehole-Formation-Rod Pump System Dynamics, including non-homogeneous zones in formation be processed.

FOR AUTHOR USE ONLY

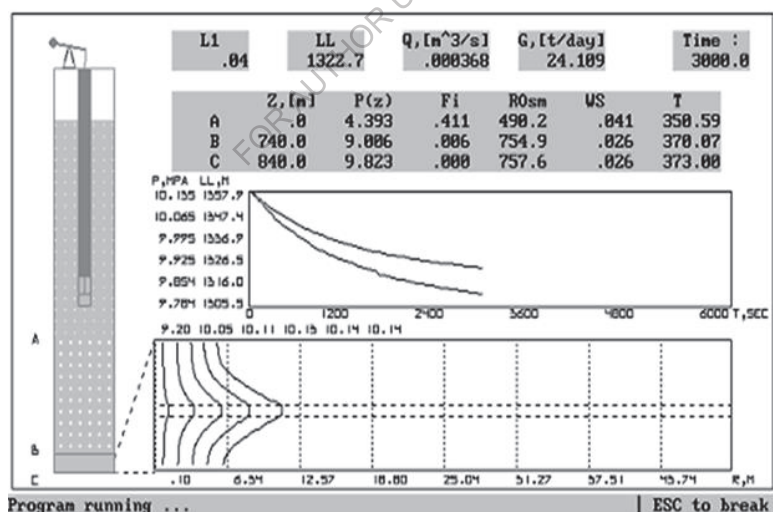
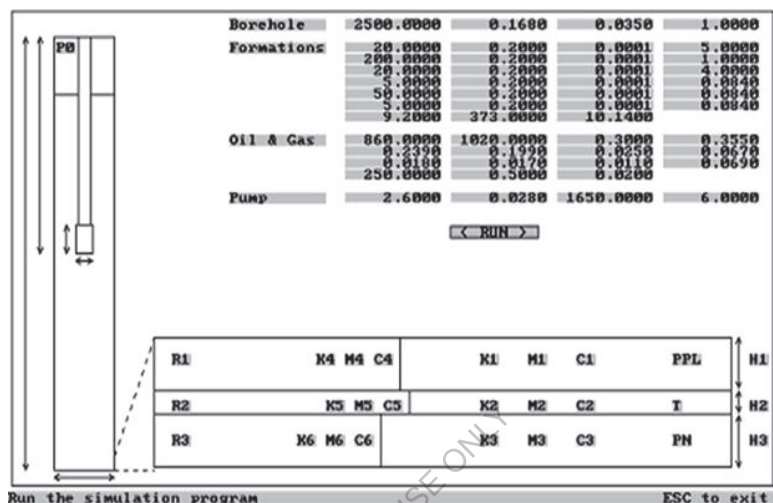


Fig.27

9. Simulator of Centrifugal Pump Optimization of Production Regime Using Borehole

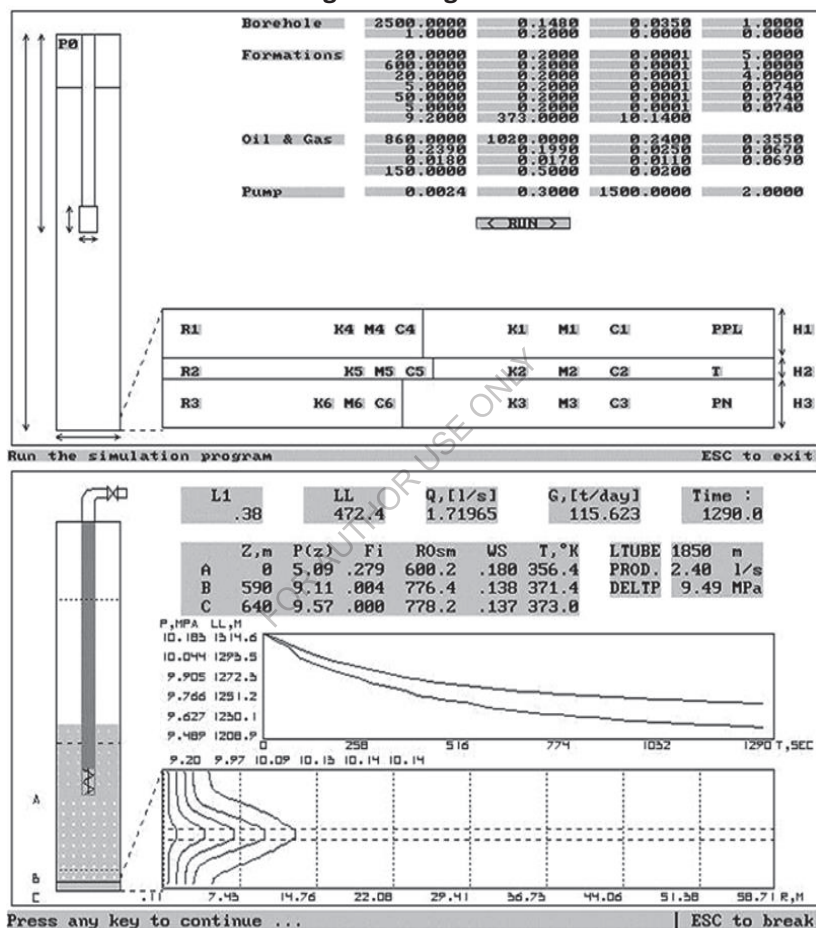


Fig.28

The simulator allows accounting for interaction between reservoir of complex structure (layered or fractured), borehole with multiphase fluid flow and a down-hole centrifugal pump. Such a consideration of the system allows more adequate simulation of processes which take place during well production.

A reservoir-borehole-pump simulator has about 45 parameters controlling the system. As the simulator takes into account filtering of a two-phase liquid through a reservoir of complex structure and flow of three-phase fluid through borehole and corresponds all three elements of the system it will maximize well production. This will allow decreasing risk of switch from production regime into gas mode for well equipped with downhole centrifugal pump. An algorithm for production optimizing was developed based on the simulation results. It allows to determine optimal location, productivity and inlet pressure of pump.

Solution is presented in graphical form with animated graphs and diagrams. Displayed values are borehole flow rate, downhole pressure, liquid level in annular space of a borehole, gas content and pressure in the point of inflow, pressure distribution in reservoir and borehole, position of the degassing level in borehole (or in reservoir), interflow distribution if reservoir is of complex structure etc.

10. Simulator of borehole-Formation-Choke System Dynamics, applied to layered formation testing

The simulator allows accounting for interaction between reservoir of complex structure (layered or fractured) and borehole with multiphase fluid flow. As a rule, the third element of the system is a two-phase choke or a down-hole pump. Such a consideration of the system allows more adequate simulation of processes which take place during formation test or well production.

A group-of-reservoirs-borehole-choke simulator has about 30 parameters controlling its elements. It allows investigating and creating methods for well production tests, for testers on tubing or logging cable accounting for their specific features. The simulator allows investigation of influence of:

- 1) reservoir properties upon apparent permeability,
- 2) degassing of oil in the zone near a borehole upon phase permeability,
- 3) perforation quality and extent upon results of measuring,
- 4) interflows between layers upon measuring,
- 5) presence of high permeability layer upon depression value near bottom,
- 6) presence of choke upon functioning of the whole system etc.

The same simulator allows to investigate the processes which take place on fountain production of a well in order to find an optimum regime of its exploitation to increase production of the well by means of changing choke diameter, proper perforation and flow rate. The simulator may also be used for theoretical researches bound with injection wells and hydraulic fracturing.

The solution is presented in graphical form on the screen being a set of isobars inside a reservoir, diagrams of bottom hole pressure and flow versus time. Optionally user can enable transit pressure curves to Simulator of Borehole-Formation-Rod Pump System Dynamics, including non-homogeneous zones in formation.

Simulation of Borehole-Formation-Nipple System Dynamics as Applied to Formation Testing

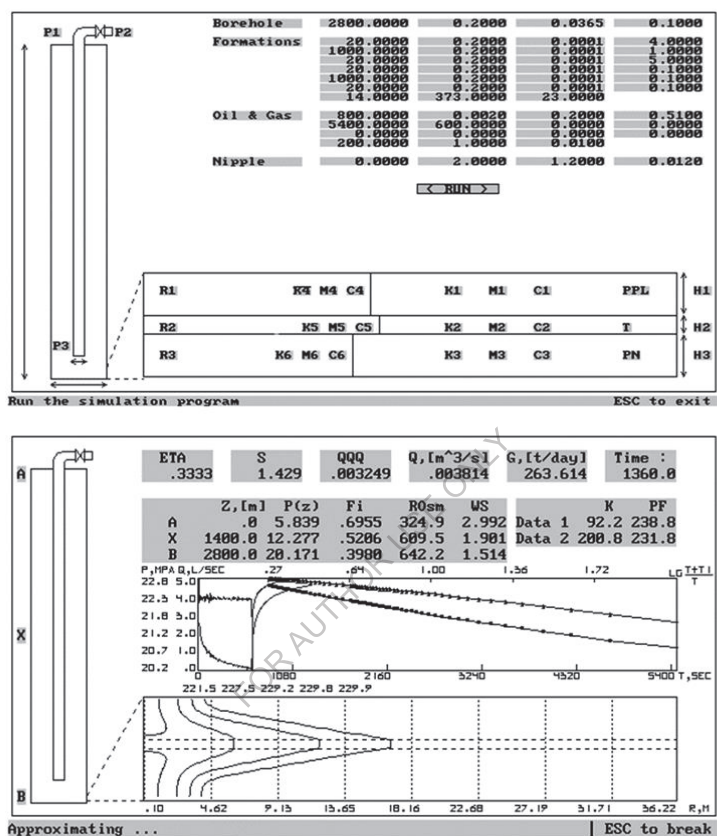


Fig.29

Abbreviations

P	- pressure, psi
So	- oil saturation
Sg	- gas saturation
Sw	- water saturation
K	- permeability, md
Koo	- relative oil permeability
Kgo	- relative gas permeability
ϕ	- porosity
μ_o	- oil viscosity
μ_g	- gas viscosity
Bo	- oil volume factor
Bg	- gas volume factor
Rs	- solution gas ratio, cft/bbl
Pf	- formation pressure, psi
Pbp	- bubble point pressure, psi
t	- time, sec
r	- radius, ft
rw	- well radius, ft
rl	- outlet radius, ft
H	- formation width, ft
Sg crit	- critical gas saturation
Qo	- oil rate, bbl/day
Qg	- gas rate, cft/day
Popt	- optimal pressure, psi

Appendix I

Article: On the Origin of Earth and Planets Magnetic Fields.

S. Tseytlin, Dr. of Sci., (Tseytlin-Consulting Inc.)

An accurate explanation of the origin of the Earth's magnetic field does not yet exist. There are several hypotheses, theories and experiments trying to find a solution to this problem, but the final, rigorous proof of these hypotheses has not been established. This article discusses the hypothesis that the main reason for the emergence and maintenance of this field are Earth's atmosphere and ionosphere. A number of estimates show the validity of this approach. Here we will give a brief summary.

1) It is well known how to determine the magnetic field of a rotating surface of a charged sphere ([1], [2]). The magnetic moment of a rotating sphere is

$$m \rightarrow = (Qa^2 \omega) / 3c$$

It is known [1] that the Earth's magnetic moment is $m = 8 \cdot 10^{25}$ units CGSE,

where $a = 6,340,000$ m - radius of Earth,

$\omega = 7.3 \cdot 10^{-5}$ 1/sec - the speed of rotation of Earth,

$c = 300,000,000$ m/sec - the speed of light.

Then, knowing the magnitude of the moment of Earth's magnetic field M , we find that the required electrical charge to generate the magnetic field is:

$$Q = 0.245 \cdot 10^{23} \text{ CGSE} = 8.1 \cdot 10^{13} \text{ C.}$$

It should be noted that a more accurate estimate of the charge, that is made on the assumption that the charge is in a spherical layer of Earth's surface and has a thickness equal to a few hundred kilometers, gives approximately the same quantity $7.5 \cdot 10^{13} \text{ C}$.

2) On the other hand, it is known (for example, [3]), that the Earth has a charge of approximately:

$$Q_{\text{earth}} = 5.7 \cdot 10^5 \text{ C.}$$

It follows that it is not enough to create Earth's magnetic field.

Suppose that there is an additional charge of a different nature, creating it. Let's find out its nature.

3) We need to pay attention to the following circumstances:

1. Only Earth has a strong magnetic field. Venus, Mars and most other planets have magnetic fields hundreds of times less.

2. Only Earth has air and water. This allows you to make the hypothesis that the Earth's magnetic field is due to the charge of the cloud layer, the value of which is enormous. It is known that the power of a lightning discharge can reach 100 Megawatt. On the other hand, there are 46 lightning discharges happening every second around the Earth.

We can estimate the charge of the clouds, assuming that the system of clouds and the ground form a spherical capacitor. Then, it is known that

$$Q_c = C \cdot U,$$

where the capacity of a spherical capacitor is:

$$C = (4\pi\epsilon_0 R_1 R_2) / (R_1 - R_2)$$

where $R_1 = 6350$ km and $R_2 = 6340$ km, R_1, R_2 - radius of the sphere and $\epsilon_0 = 8.85 \cdot 10^{-12}$,

It should be noted that, given that dielectric constant of water is 80, the capacity of the cloud layer may be higher by one or more orders.

Then we see that capacity is approximately:

$$C = (0.45 \div 4.5) \text{ Farads.}$$

We estimate the potential voltage U between the clouds and the Earth's surface. Let's assume the voltage of air breakdown $E = (10 \div 30)$ Kvolt/cm. Then $U = E \cdot H = 3 \cdot 10^6 \cdot H$ Volt, where $H = (1 \div 10) \cdot 10^3$ m - height of the clouds.

The result is an upper bound of the charge of the clouds of Earth:

$$Q_{1 \text{ max}} = C \cdot E \cdot H = 4.5 \cdot 3 \cdot 10^6 \cdot 10^4 = 1.35 \cdot 10^{11} \text{ C.}$$

However, it should be noted that deposits of iron and nickel in the upper part of the crust could increase this magnetic field.

Which proves that the charge of the clouds can create a sufficiently strong magnetic field comparable with the Earth's magnetic field.

4) Another estimate of Earth's magnetic field gives approximately the same result.

The fundamental work of A. Karelin estimated the charge density of thunderclouds [4].

Distribution of lightning on the Earth's surface.

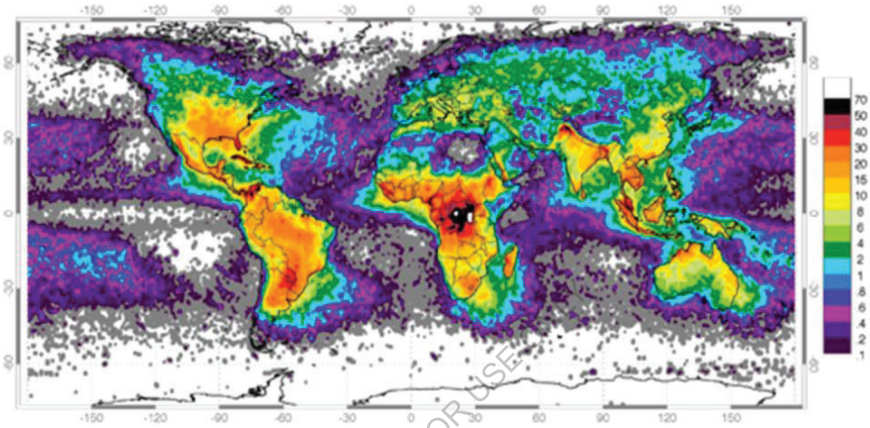


Fig. 1

At every given moment on Earth there are about 1500 storms. The average frequency of lightning discharge is estimated as 46 per second. Storms are unevenly distributed on the planet's surface.

As a result, there is given calculations and experiments, the density of the charge is in the range $q = (9\text{--}280) \cdot 10^{-9} \text{ C / m}^3$. Then, taking the amount of cloud cover in the form $V = 4\pi \cdot R_2 \cdot H$, where $H = 1000 \text{ m}$ - thickness, we get

$$V = 50 \cdot 10^{17} \text{ m}^3$$

Then we obtain an estimate of the charge of storm clouds on Earth, which varies in the range of

$$Q_1 = V \cdot q = (4.5\text{--}140) \cdot 10^{10} \text{ C}.$$

If the area of the storm clouds takes up one-tenth of the sky, and they have the lowest charge density, we get a lower estimate of the charge equal to

$$Q1 \text{ min} = 4.5 \cdot 10^9 \text{ C.}$$

The highest estimate will be equal to

$$Q1 \text{ max} = 1.4 \cdot 10^{11} \text{ C.}$$

which practically coincides with the estimate obtained in the previous section.

The procedure of this evaluation indicates that the charges of Earth's atmosphere can be a major source of Earth's magnetic field. However, they are not enough. Additional contributions can give the effect of the location of the iron in the Earth's crust and charges are in the Earth's ionosphere.

5) One of the missing links in determining the Earth's magnetic field may be the effect of the upper layer of the earth's crust to a depth of 15 kilometers, where lie the iron and nickel deposits, which have a temperature below the Curie temperature. enormous deposits of iron and nickel (which make up 5% of the total weight of the crust of the earth and at 30% of its volume), which may influence the magnitude of the magnetic field of the Earth, increasing it a few times. Note that the total amount of iron in the world has changed for all its life, as part learned from her, it is on its surface and in its interior portion. It changed only their relationship.

6) Offer a theory of occurrence of Earth's magnetic field explains the presence and magnitude of the magnetic field close to Earth planets.

This is especially Venus. Venus is the most Earth-like planet that does not have a strong magnetic field, but the internal structure of their identity. Venus has an atmosphere and ionosphere consisting mainly of CO₂ gas, which has a certain capacity and who are constantly recharged by the solar wind like Earth. It should also be noted that the length of day Venus more than 243 times greater than the Earth. The rate of motion of the charges in the ionosphere of Venus is hundreds of times slower than in the Earth's ionosphere, which explains why the magnetic field of Venus is less than the magnetic field of the Earth in 300 or even more times.

Consider Mercury. It is well known that its magnetic field is more than a hundred times smaller than the Earth. On the other hand, the length of his day is less to 58 times then Earth, and his radius is 2440 km. Than the velocity of the negative charges in the ionosphere of Venus is 152 times slower than the Earth's

ionosphere. This may explain the decrease in its magnetic field, as compared to the Earth.

The site: <https://sites.google.com/site/astronom1543/mag>

indicated that the measurement of the magnetic field of Mercury is 0.006 of the magnetic field of the Earth, that is 150 times smaller than that coincides with our assessment!

Let's consider now the magnetic field of Jupiter. It is known that Jupiter has a magnetic field approximately 20 times greater than the Earth. It is known that the radius of Jupiter is 11 times greater than the radius of the Earth, and the rotational speed is 2.4 times greater. So the velocity of the charges in the ionosphere of Jupiter is 26.4 times greater than the Earth's ionosphere. Measurements have shown that the magnetic field of Jupiter is 20-50 times greater than the magnetic field of the Earth. In this case, the magnetic field of Jupiter Rated via offers theory also gives good agreement with the measurement!

Only Mars is not subject to the laws are risen. The magnetic field of Mars is extremely small - more than 500 times weaker than the magnetic field of Earth. The size of Mars and its rotational speed is almost completely coincided with the Earth. Therefore, all the conditions for the operation of the mechanism same hydrodynamic dynamo must be similar create magnetic fields. However, the difference in the observed magnetic field is due to the actual current lack of Mars's atmosphere and ionosphere. The pressure of the atmosphere at the surface of Mars is 160 times smaller than the Earth. This proves that the source of the magnetic field depends on the presence of the ionosphere, because the rest of the parameters of the planets almost are same. Analysis of tectonic rocks shows that when the magnetic field of Mars was quite noticeable and had reversal of the magnetic field. We know that the destruction of the Marsian atmosphere is relatively recent and continues to be now. The lack of atmosphere and magnetic field are the main reason for the absence of life on Mars, but does not rule out its existence in the past. There are several hypotheses causes destruction of the Martian atmosphere, but we will not dwell on them. The fact is that in the absence of an atmosphere and the ionosphere notable planet's magnetic field cannot exist.

Thus, the connection of existence of magnetic fields of the planets with their ionosphere is another proof that the reason for their existence hydrodynamic dynamo mechanism is not because in a Mars hydrodynamic dynamo mechanism, located inside the planet would have to continue to work and create a magnetic field commensurate with the Earth's magnetic field.

We will build a Tab.1

<i>Planet</i>	<i>Diameter</i>	<i>rotation</i>	<i>mag. field</i>	<i>Atmos. pressure</i>
Mercury	4879	58.8	0.006	0.001
Venus	12104	243.7 93	0.003	93
Earth	12742	1	1	1
Mars	13558	1.01	0.002	0.06
Jupiter	139 822	9.92	25	12

Tab.1

From Table 1 the following conclusions:

- 1) Where there is no atmosphere and ionosphere of the magnetic field, or negligible, if any, it almost does not (Mercury, Mars).
- 2) From the Earth and Mars comparing seen that the dimensions and rotational speed are nearly the same. Time and conditions of occurrence should be almost identical. Therefore, if there was a valid hypothesis on the origin of magnetic fields thanks to the mechanism of hydrodynamic dynamo, then they would have been identical to the magnetic field. But it is not! So, the hypothesis of the origin of Earth's magnetic field through the mechanism of hydrodynamic dynamo is incorrect.
- 3) Radiuses and speeds of the planets determine the velocity of the charges in the ionosphere. And hence the current.

Then those planets that have an atmosphere and ionosphere country powered according to our hypothesis from the solar wind should be proportional to the magnetic field of the linear velocity of the ionosphere, so multiply of the radius by the angular speed! Indeed Venus, which has a radius slightly smaller than

Earth, but with a smaller rotating 243 times the speed of a magnetic field nearly 300 times smaller. Jupiter, which has a radius of 11 times larger than the Earth and rotating with an angular velocity of 2.4 larger than the Earth's magnetic field is 25 times greater. **These estimates confirm the correctness of our hypothesis that the mechanism of borrowing and the Earth's magnetic field is produced by moving charges ionosphere created by solar wind.**

Hence, our hypothesis is the emergence and existence of the Earth's magnetic field has more reason than hydrodynamic dynamo hypothesis than its origin.

7) Note that offers a hypothesis about the cause of Earth's magnetic field makes it easy to explain not only the origin of the Earth's magnetic field, but the geomagnetic Inversion, that occurs every few hundred thousand years is stochastic.

Analysis of the Earth's magnetic field, conducted with the help of satellites and modeling has shown that the solar wind is currently bears, because it mainly content electrons negative charge. In case of a positive charge in the solar wind and Earth's magnetic poles form of distortion of the magnetic field of the Earth, associated with the existence of wind would have been different.

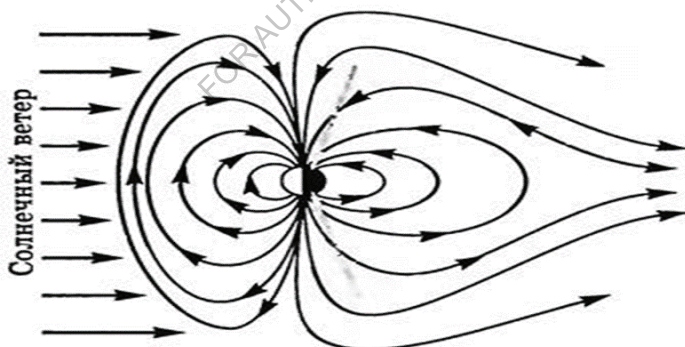


Fig.2

Solar prominences - a charged plasma field, recurring over the surface of the Sun, overcome gravity and the magnetic attraction of the sun, pulled out from the surface of the sun. And partly substance prominences back into the sun, and some in the form of solar wind scatters in different directions. Part of this wind reaches

the Earth's ionosphere and charges negative charge. The ionosphere exists the so-called E and F layers [6] located in the region of 90 to 500 km long and having electrons in a concentration range of $N_e = (1.5\text{--}30) \cdot 10^5$ in one cubic centimeter (3) formed through Sunny wind. The average value of the electron density in them is $N_e = 10^6$.

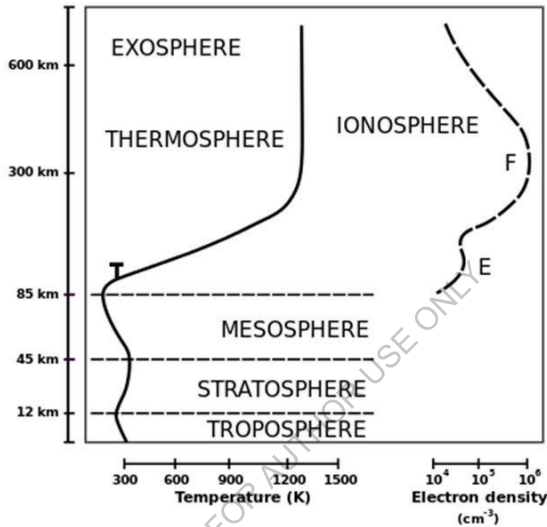


Fig. 3

All thickness of these layers up to $H = 500$ km. Then it is easy to estimate the total charge of this layer. It is

$$Q_{\text{earth}} = Q_e \cdot R^2 \cdot 4\pi N_e \cdot H = 4.14 \cdot 10^{13} \text{ C}$$

Where $Q_e = 1.6 \cdot 10^{-19}$ C electron charge.

As the assessment conducted by a charge E + F layer of the ionosphere, considering the effect of the iron contained in the upper layer of the Earth, its size is sufficient to establish, or at least make a major contribution to the formation of Earth's magnetic field.

It should be noted that the constant losing due to the negative charge of this leads to the fact that periodically, every few hundred thousand years, the sun begins to

break out of the positively charged gigantic prominences (predominantly due to their content of positive ions and protons), dimensions reach several thousand kilometers. Therefore, the solar wind starts bearing positive charges which reach Earth and recharge its electric and magnetic field.

As a result, through some period equal several thousand, the Sun again becomes neutral and starts letting out negatively loaded wind again.

The next inversion of the Magnetic Field of Earth results. The recharge of the Magnetic Field of Earth can occur as well as a result collision of Earth with huge comets which can be loaded both is negative, and is positive, depending on a sign of a charge of a star which the comet faced before it.

So, process of inversion of the Magnetic Field of Earth can be explained easily on the basis of the offered hypothesis.

8) Now we will stop briefly on other approaches to an explanation of emergence of the Magnetic Field of Earth. First of all, we will note that now on the first place for an explanation of emergence of the Magnetic Field of Earth by other authors the mechanism connected with the thermal convection in its liquid magma is considered. Such hypothesis is based on analogy of the mechanism of emergence and maintenance of a magnetic field of the Sun.

However, the simple analysis shows that in the conditions of Earth this mechanism can't work because of a difference of scales and sizes of density and viscosity of the fluids and gradients of temperature existing on the Sun and Earth. It is known that the big gradient of temperatures and existence of an easy non viscous fluid in the studied volume is necessary for the noticeable thermal convection. But change of temperature of terrestrial magma from the top part adjoining on bark and equal 700 degrees, and lower, adjoining on a kernel of equal 6000 degrees at distance about 3000 km, gives the top assessment of a gradient - 2 degrees on kilometer. It is less than in bark of Earth and considering that viscosity of magma, even at a temperature of 4000 degrees the very high – it is possible to draw a conclusion that UNDER THESE CONDITIONS in Earth there CAN not be a CONSIDERABLE THERMAL CONVECTION!

It should be noted also that fact that maintenance of a magnetic field of Earth requires huge energy. As any electromagnetic generator has to use the rotating

rotor which role plays the Earth globe. Thus, there are forces and inductive currents breaking it. It is required or additional the energy maintaining constancy of speed of its rotation, or it has to slow down, losing rotation speed. Practice of supervision shows – the speed of rotation of Earth for millions of years almost didn't change.

So, in Earth there are no sufficient sizes of parameters that there were conditions necessary for operation of the mechanism of a hydro magnetic dynamo.

For comparison, on the Sun temperature changes from 6000 to 15 000000 degrees, and the fluid represents plasma (the ionized gas) which density is one hundred times less than magma density, and viscosity of magma one thousand times smaller than viscosity. Under these conditions there can be strong magnetic fields thanks to the mechanism of a hydrodynamic dynamo.

9) It is possible to prove correctness of the version that sources of the Magnetic field of Earth are out of its volume, simpler way. It is known how it was already noted that in Earth bark at depths up to about 15 kilometers where being carried out by a condition of that temperature is less than Curie's point, fields of iron and nickel making about of 5% of bark volume lie. It is known also that the Magnetic Field of Earth measured along its surface, then value of the Magnetic Field of Earth in regions of its bedding. In case of an arrangement of charges and currents over Earth surface, the effect has to be opposite since metal plays a role of the paramagnetic internal core and the magnetic field has to increase around its bedding! As it was mentioned above, practice of measurement of the Magnetic Field of Earth showed names it. Therefore, the version about finding of sources of the Magnetic Field high – it is possible to draw a conclusion that UNDER THESE CONDITIONS in Earth there CAN not be a CONSIDERABLE THERMAL CONVENTION!

It should be noted also that fact that maintenance of a magnetic field of Earth requires huge energy. As any electromagnetic generator has to use the rotating rotor which role plays the Earth globe. Thus, there are forces and inductive currents breaking it. It is required or additional the energy maintaining constancy of speed of its rotation, or it has to slow down, losing rotation speed. Practice of supervision shows – the speed of rotation of Earth for millions of years almost didn't change.

So, in Earth there are no sufficient sizes of parameters that there were conditions necessary for operation of the mechanism of a hydro magnetic dynamo.

For comparison, on the Sun temperature changes from 6000 to 15 000000 degrees, and the fluid represents plasma (the ionized gas) which density is one hundred times less than magma density, and viscosity of magma one thousand times smaller than viscosity. Under these conditions there can be strong magnetic fields thanks to the mechanism of a hydrodynamic dynamo.

9) It is possible to prove correctness of the version that sources of the Magnetic field of Earth are out of its volume, simpler way. It is known how it was already noted that in Earth bark at depths up to about 15 kilometers where being carried out by a condition of that temperature is less than Curie's point, fields of iron and nickel making about of 5% of bark volume lie. It is known also that the Magnetic Field of Earth measured along its surface, then value of the Magnetic Field of Earth in regions of its bedding. In case of an arrangement of charges and currents over Earth surface, the effect has to be opposite since metal plays a role of the paramagnetic internal core and the magnetic field has to increase around its bedding! As it was mentioned above, practice of measurement of the Magnetic Field of Earth showed names it. Therefore, the version about finding of sources of the Magnetic Field of Earth out of Earth surface is fair. And consequently, the version and the carried-out estimates about location of these sources in the atmosphere and an ionosphere of Earth the correct.

10) We will note that by means of the offered hypothesis it is easy to explain discrepancy of a geometrical axis of Earth and an axis of a magnetic field of Earth. (Shift of magnetic poles).

This phenomenon arises because of an inclination of a geometrical axis of Earth to Earth orbit plane on 23.4 degrees. In this connection the solar wind falls on Earth surface at an angle.

11) Thus, only the charges brought from the outside (A solar wind or comets) and the charges resulting from formation of drops of a rain in clouds can constantly load the atmosphere and an ionosphere, allowing to create and support the Magnetic Field of Earth.

And the magnetic field of the atmosphere of Earth can serve as a starter of emergence of the Magnetic field of Earth, originally braking and developing electrons of the Solar wind on a tangent to Earth surface.

The carried-out estimates showed that the total charge of Earth, clouds and an ionosphere can provide emergence and existence of the Magnetic field of Earth. And the charges arising in atmosphere clouds constantly are supported by a water circulation in the nature, and an ionosphere charge, is constantly recharged by the streams of charged particles coming from the Sun.

Bibliography

1. Electrician and Electrician, 2010, No. 6, or3. "Physical quantities", Reference book, M. Energoizdat, 1991, p. 1196, or Capstones in Physics: Electromagnetism ©1999 Oregon State University, P. Siemens
4. Questions electricians T. 118. 2010, p. 45-49, Karelin A.V. MECHANISM OF GENERATION OF ELECTRICITY In STORM CLOUDS AND TROPICAL HURRICANES or The electrical nature of storms/D.R. MacGorman, W.D. Rust. – Oxford: Oxford Univ. Press, 1998. – 380 p.
5. Venus, From Wikipedia, free encyclopedia
6. Wikipedia, free encyclopedia, Ionosphere. Physics for Scientists and Engineers, Volume 2 By Raymond Segway, John Jewett
7. The magnetic moment of the rotating sphere, Roman Parpolak. Or Griffiths, David J. (2007) Introduction to Electrodynamics, 3rd Edition; Prentice Hall – Chapter 5, Post 36

FOR AUTHOR USE ONLY

**More
Books!**

yes
I want morebooks!

Buy your books fast and straightforward online - at one of world's fastest growing online book stores! Environmentally sound due to Print-on-Demand technologies.

Buy your books online at
www.morebooks.shop

Kaufen Sie Ihre Bücher schnell und unkompliziert online – auf einer der am schnellsten wachsenden Buchhandelsplattformen weltweit! Dank Print-On-Demand umwelt- und ressourcenschonend produziert.

Bücher schneller online kaufen
www.morebooks.shop

KS OmniScriptum Publishing
Brivibas gatve 197
LV-1039 Riga, Latvia
Telefax: +371 686 204 55

info@omniscryptum.com
www.omniscryptum.com

OMNIScriptum



FOR AUTHOR USE ONLY